Supporting Information

Self-sensitized Cu(II)-Complex Catalyzed Solar Driven CO_2 Reduction

Soumadip Das, Aritra Roy, Navonil Chakrabarti, Narottam Mukhopadhyay, Aniruddha Sarkar and Sayam Sen Gupta*
Department of Chemical Sciences, Indian Institute of Science Education and Research Kolkata, Mohanpur, 741246, India
*Email: sayam.sengupta@iiserkol.ac.in

Contents:

EXPERIMENTAL SECTION

1. Materials and Methods:

All materials were commercially purchased and used without further purification unless otherwise mentioned. Pyrrole-2-carboxylic acid, HATU, and p-nitrobenzaldehyde were purchased from BLDpharma. N, N-diisopropylethylamine, and Pivaloyl Chloride were purchased from Spectrochem. 4-isopropylaniline, 18-crown-6, was purchased from TCI Chemicals. Pd/C, DDQ, and anhydrous $CuCl_2$, KH were purchased from Sigma Aldrich. THF, Acetonitrile, N, N-dimethylformamide, Hexane, Diethyl Ether, and Toluene were purchased from Merck and used after distillation over corresponding drying agents[1]. For metalation, double-distilled, sodium-dried THF was used. For manipulation of the metal complex, acetonitrile was double-distilled and used. For thin-layer chromatography (TLC) analysis, Merck precoated TLC plates (silica gel 60 F254/0.25 mm) were used.

2. Instrumentation:

UV-vis spectral studies were carried out using an Agilent diode array Cary 8454 spectrophotometer (190-1100 nm range. Room temperature solution state emissions were performed with a Fluoromax3 spectrofluorometer from Horiba Jobin Yvon. The TCSPC measurements were recorded using a Horiba DeltaFlex-01 TCSPC spectrometer (l_{ex} = 405 nm). The instrument response function (IRF) of the instrument used for fluorescence lifetime measurement is 100ps. DLS measurements were carried out using Malvern Zetasizer NanoZS. Mass spectral analyses were done in a Bruker micrOTOF-Q II spectrometer and Waters-HAB213 spectrometer. ^{1}H and ^{13}CNMR spectra were collected using Bruker (^{1}H: 500 MHz, ^{13}C: 126 MHz) referenced to the resonances of the solvent used. Glassy Carbon, Pt, and Ag/AgCl (aqueous) electrodes were purchased from CH Instruments. All the cyclic voltammetry studies were carried out in CHI-660 potentiostat. Electron Paramagnetic Resonance (EPR) spectroscopy was studied by a Bruker spectrometer (Bruker, EMXmicro) operating at X-band frequency (Microwave frequency 9.32 GHz) and magnetic field modulation of 100 kHz, with a microwave power of 48.83 mW and modulation amplitude of 10 G at low temperatures. The EPR spectra were calibrated with diphenylpicrylhydrazyl, DPPH (g = 2.0037). Parameters at which this EPR was recorded are as follows- vMW = 9.31 GHz (3.2 mW), 10 G field modulation (100 kHz), receiver gain = $2x10^2$, time constant = 81.92 ms, conversion time = 150ms (80 K). Spectra were treated using Bruker WinEPR software and simulated using Bruker SIMFONIA software. Kessil lamp (model: PR160L-390 nm) and (model: PR160L-427 nm) were used for photo-irradiation on the reaction mixture. Gas Chromatography (GC) was performed on a Thermo Scientific Carbon plot gas chromatograph using a DB-5 ms capillary column (30 m × 0.25 mm × 0.25 µm, J&W Scientific) with helium as the carrier gas. FTIR Perkin-Elmer spectrophotometer was used to obtain the FT-IR spectra.

2. Quantum Chemistry Calculation:

The DFT optimization was performed using Gaussian 16.[2] The geometry optimizations, molecular orbital, and TDDFT calculation of the ground state structures were carried out using unrestricted B3LYP as a function.[3,4] Geometries were optimized without constraints and confirmed as local minima through a frequency analysis with the basic set LANL2DZ for copper and 6-311G+* on the rest of the atoms.[5,6] All calculations were run with a solvent model (SMD) with a dielectric constant mimicking acetonitrile. Molecular orbital optimization and TDDFT calculation were performed with basis set LANL2DZ for copper and 6-311G+* on the rest of the atoms.

3. Crystal Structure Determination:

Single crystals of suitable dimension were used for data collection. Diffraction intensities were collected on a XtaLAB Synergy, Dualflex, HyPix3000, four-circle diffractometer (Department of Chemical Sciences, IISER Kolkata, India), with graphite monochromated Cu-Kαradiation (l = 1.54184 Å) at 100(2) K for **2**−**4**. The data were corrected for absorption. For data reduction, the 'Bruker SAINT PLUS' and 'CrysAlisPro 1.171.41.93a' programs were used. Data were corrected for Lorentz and polarization effects; empirical absorption corrections (SADABS v 2.10) were applied. The structures were solved by SHELXT and refined with the SHELXL**–**2016 package,[7] incorporated into the Olex2 1.2.8**–**alpha crystallographic collective package.[8,9] All crystal structures are represented by the MERCURY program.[10] The positions of the hydrogen atoms were calculated by assuming ideal geometries but not refined. All non-hydrogen atoms were refined with anisotropic thermal parameters by full-matrix least-squares procedures on F^2. Pertinent crystallographic parameters are summarized in **Table S1** (for **1** at 100(2) K).

4. Electrochemical Measurement (Homogeneous):

Cyclic voltammetry experiments were performed to investigate the redox potential of the ligand and the complex. Glassy carbon was used as a working electrode, an Ag/AgCl (saturated KCl, aq.) was used as a reference, and a Pt wire was used as a counter electrode. All electrochemical measurements were performed in acetonitrile, and tetrabutylammonium hexafluorophosphate ($TBAPF_6$) was used as a supporting electrolyte. The electrolytic solution was saturated with Ar or CO_2, as mentioned. Ferrocenium/Ferrocene (Fc^+/Fc) couple was used as an internal standard against which all data has been standardized.

5. Fluorescence Quenching:

In a sealed quartz cuvette with a septum cover, a solution of **1** was taken in Ar-degassed acetonitrile. The solution received additions of varying concentrations of Et_3N. The steady-state fluorescence was measured using a Horiba Fluoromax 4 spectrofluorometer. The excited state lifetime (τ_0) of **1** was measured with a nanosecond pulse diode laser (λ=405nm) was used as the excitation source. The quenching rate constant (k_q) was calculated by the Stern-Volmer equation:

$$\frac{I_0}{I} = 1 + k_q \times \tau_0 \times [Q]$$

Where, I_0 and I represent the fluorescence intensity of photosensitizer in the absence and presence of a quencher, k_q is the quenching rate constant, and [Q] is the concentration of the quencher.

6. Photocatalytic CO_2 Reduction:

The Photocatalytic experiments were conducted in an air-tight 15ml test tube with a rubber septum and were accompanied by magnetic stirring. The headspace of the vial was 12mL. A reaction mixture (3.0 mL) was bubbled with CO_2 for 40 min and then irradiated with a Xe light setup (I > 400 nm)/ 390nm (Kessil lamp model: PR160L) and 427 nm (Kessil lamp model: PR160L). The gas detected with Gas Chromatography (GC) was performed on a Thermo Scientific Carbon plot gas chromatograph using a DB-5 ms capillary column (30 m × 0.25 mm × 0.25 µm, J&W Scientific) with helium as the carrier gas.

7. General Procedure for the Synthesis of NDPA (H_3L) Ligand:

A. *Synthesis of N-(4-isopropylphenyl)-1H-pyrrole-2-carboxamide (**A**):*

Pyrrole-2-carboxylic acid (1gm, 9mmol) and HATU (4.11gm, 10.8mmol) were added to a two-neck round bottom flask under an N_2 atmosphere. 10 mL of DMF was added to this mixture, followed by DIPEA (4.7mL, 27mmol). This was allowed to stir at room temperature for 30 minutes. 4-isopropylaniline (2.46mL, 18mmol) was added dropwise to this solution. The resultant mixture was stirred at room temperature for 8 hours. The organic layer was extracted in DCM and washed with 2(M) HCl, saturated aqueous sodium bicarbonate solution, and brine. The title compound was purified by column chromatography in ethyl acetate-hexane as the eluent and yielded a white crystalline solid. (1.63gm, 7.14mmol). Yield: 79.3%

^{1}H NMR (500 MHz, $CDCl_3$): **d** 9.83 (s, 1H), 7.60 (s, 1H), 7.51 (d, *J* = 7.5 Hz, 2H), 7.21 (d, *J* = 8.5 Hz, 2H), 6.98 (s, 1H), 6.71 (s, 1H), 6.28 (s, 1H), 2.90 (hept, *J* = 6.9 Hz, 1H).

^{13}C NMR (126 MHz, $CDCl_3$): **d** 159.47, 145.38, 135.78, 127.37, 126.46, 122.69, 120.62, 110.47, 109.74, 34.00, 24.42.

B. *Synthesis of 5,5'-(phenylmethylene)bis(N-(4-isopropylphenyl)-1H-pyrrole-2-carboxamide) (**B**):*

(A) (1gm, 4.38mmol) and p-nitrobenzaldehyde (315.2mg, 2.09mmol) were taken in a two-neck round bottom flask. To this was added a catalytic amount of PTSA (~5mg) and refluxed in a Dean-Stark setup for 6h, yielding a pink precipitate. This was allowed to cool to room temperature, filtered, washed repeatedly with n-hexane, and dried under vacuum to yield a pink solid. (1.13gm, 1.92mmol) Yield: 91.87%

^{1}H NMR (500 MHz, DMSO-d^6): **d** 11.74 (s, 2H), 9.66 (s, 2H), 8.20 (d, *J* = 8.6 Hz, 2H), 7.61 (d, *J* = 8.5 Hz, 4H), 7.43 (d, *J* = 8.7 Hz, 2H), 7.18 (d, *J* = 8.4 Hz, 4H), 7.01 (s, 2H), 5.93 (s, 2H), 5.81 (s, 1H), 2.84 (p, *J* = 7.0 Hz, 2H), 1.18 (d, *J* = 7.0 Hz, 12H).

^{13}C NMR (126 MHz, DMSO-d^6): **d** 158.96, 150.15, 146.13, 143.03, 137.01, 136.12, 129.38, 126.28, 126.02, 123.48, 120.05, 111.39, 108.51, 59.75, 42.57, 32.88, 23.98, 20.76, 14.09.

C. *Synthesis of 5,5'-((4-aminophenyl)methylene)bis(N-(4-isopropylphenyl)-1H-pyrrole-2-carboxamide) (**C**):*

(B) (1gm, 1.70mmol) was dissolved in dry THF, and 10% Pd/C (18mg) was added. The mixture was saturated with H_2 and stirred at room temperature for 4h. The Pd/C was then removed by filtration, and the solvent was removed in vacuo. The residue was washed with ether to give (3) an off-white solid. The next step was proceeded without further purification.

D. *Synthesis of 5,5'-((4-pivalamidophenyl)methylene)bis(N-(4-isopropylphenyl)-1H-pyrrole-2-carboxamide) (**D**):*

(C) (750mg, 1.34mmol) was dissolved in dry THF in a two-neck round bottom flask under N_2. This was cooled to 0°C, followed by the addition of triethylamine (205.45µL, 1.47 mmol). Pivaloyl Chloride was added (196.83µL, 1.61 mmol), and the mixture was allowed to stir at 0°C for 15 minutes. Then it was allowed to come to room temperature and was stirred for 12h until a white precipitate of triethylamine hydrochloride was formed, and the solution turned orange. The solid was filtered off, and the organic layer was extracted in ethyl acetate and washed with 2(M) HCl, saturated aqueous sodium bicarbonate solution, and brine to give a light orange solid (D), which was further purified by column chromatography. (702mg, 1.09mmol) Yield: 81.37%

^{1}H NMR (500 MHz, DMSO-d^6): **d** 11.53 (s, 2H), 9.90 (s, 1H), 9.60 (s, 2H), 7.60 (d, *J* = 8.7 Hz, 4H), 7.50 (d, *J* = 8.7 Hz, 2H), 7.17 (d, *J* = 8.7 Hz, 4H), 7.11 (d, *J* = 8.9 Hz, 2H), 6.97 – 6.94 (m, 2H), 5.88 – 5.85 (m, 2H), 5.56 (s, 1H), 2.83 (p, *J* = 6.9 Hz, 2H), 2.02 (s, 3H), 1.18 (d, *J* = 6.9 Hz, 12H).

^{13}C NMR (126 MHz, DMSO-d^6): **d** 168.30, 159.14, 143.11, 137.96, 137.24, 128.49, 126.43, 125.68, 120.15, 119.04, 111.62, 108.21, 42.50, 33.02, 25.29, 24.14.

E. *Synthesis of (Z)-N-(4-isopropylphenyl)-5-((5-((4-isopropylphenyl)carbamoyl)-2H-pyrrol-2-ylidene)(4-pivalamidophenyl)methyl)-1H-pyrrole-2-carboxamide (NDPA) (**H_3L**)*

(D) (2gm, 3.11mmol) was dissolved in dry THF in a two-neck round bottom flask under an inert atmosphere. This was allowed to cool to 0°C. DDQ (846.18mg, 3.73mmol) was weighed and dissolved in dry THF under an inert atmosphere in another two-neck round bottom flask. Following this, the DDQ solution was added dropwise over a period of 30 minutes to (D) until the color changed from orange to deep purple and eventually dark red. The mixture was allowed to come to room temperature and stirred for 4h. The THF was removed in vacuo, and the organic layer was extracted in ethyl acetate and washed with saturated aqueous sodium bicarbonate solution and brine to yield a bright red solid. This was further purified by column chromatography in neutral alumina media, with ethyl acetate-hexane as the eluent. The title compound was eluted as a bright red band and was dried in vacuo to give a fine red powder (1.77g, 2.76 mmol). Yield: 88.93%

^{1}H NMR (500 MHz, DMSO-d^6): **d** 11.58 (d, *J* = 5.2 Hz, 2H), 9.64 (s, 2H), 9.20 (s, 1H), 7.64 (d, *J* = 8.5 Hz, 4H), 7.60 (d, *J* = 8.7 Hz, 2H), 7.18 (d, *J* = 8.7 Hz, 4H), 7.14 (d, *J* = 8.7 Hz, 2H), 7.00 (s, 2H), 5.89 (s, 2H), 5.60 (s, 1H), 2.84 (hept, *J* = 6.9 Hz, 2H), 1.23 (s, 9H), 1.19 (d, *J* = 6.9 Hz, 12H).

^{13}C NMR (126 MHz, DMSO-d^6): **d** 177.08, 159.36, 149.34, 145.73, 144.11, 141.05, 136.53, 131.92, 130.44, 126.62, 125.06, 120.18, 119.03, 107.14, 33.11, 30.58, 27.29, 23.72.

HR-MS: 642.3446 $[M+H]^+$

F. *Synthesis of deprotonated NDPA ligand (**L^{3-}**):*

100mg of NDPA(H_3L) (155.81µmol) was taken into a Schlenk tube inside the glove box and dissolved in ~8ml of Na-dried THF. To this orange solution, KH (3.3 eq., 514 µmol) was added. The color immediately changes to dark pink with the evolution of hydrogen. It was kept for 4h of stirring. For all the UV-vis and fluorescence studies, 3eq. of 18-Crown-6 (467.43 µmol) was added into the solution to stabilize the trianionic ligand.

^{1}H NMR (500 MHz, DMSO-d^6): **d** 7.32 (s, 1H), 7.21 (d, *J* = 8.7 Hz, 4H), 7.08 (d, *J* = 8.5 Hz, 2H), 6.88 (d, *J* = 8.5 Hz, 1H), 6.78 (d, *J* = 8.7 Hz, 4H), 6.61 (s, 1H), 6.39 (s, *1*H), 6.13 (s, 1H), 5.74 (s, 1H), 5.61 (s,1H), 2.70 (m, 2H), 1.13 (d, *J* = 6.9 Hz, 12H), 1.07 (s, 9H).

8. General Procedure for the Synthesis of K[CuNDPA] (Complex 1):

100mg of NDPA (**H_3L**) (155.81µmol) was weighed into a Schlenk round bottom flask inside the glove box and dissolved in ~8mL of Na-dried THF. To this orange solution, KH (3.3 eq., 514 µmol) was added. The color immediately changed to dark pink with the evolution of H_2. This was left to stir for 30 minutes, followed by the addition of anhydrous $CuCl_2$ (20.95mg, 155.81 µmol). Immediately, the color changed to dark purple. After

stirring it under an inert atmosphere for 4 hours, the solution was filtered inside the glove box. The residue was solvated in dry, distilled acetonitrile, which separated the metal complex from the unreacted $CuCl_2$. The resulting solution was bright purple, and the solvent was removed by dry distillation to yield a purple-colored solid (79mg, 112.48 µmol). This complex was taken in acetonitrile, and 1.1 eq. of 18-crown-6 was added to this purple solution. A single crystal was obtained in acetonitrile diffused with Et_2O. Yield: 72.19%

Analytical Calculation for C52H64CuKN5O9(**1**) f_w=1004.3637: (*expected*) C= 62.10, H= 6.41, N= 6.96; (*observed*) C= 61.71, H= 6.45, N= 6.91

UV-vis (in CH_3CN): λ, nm (ε, M^{-1} cm^{-1}): 378nm (13042 M^{-1} cm^{-1}), 558nm (8079M^{-1} cm^{-1}), 598nm (8437M^{-1} cm^{-1})

HR-MS: 701.27 $[M]^-$

9. General Procedure for the Synthesis of CuNDPA with N_2O_2 coordination (Complex 3):

100mg of NDPA (**H_3L**) (155.81µmol) was weighed into a round bottom flask and dissolved in ~8mL of Na-dried THF. To this orange solution, anhydrous $CuCl_2$ (20.95mg, 155.81 µmol) was added. Immediately, the color changed to dark red. After refluxing it for 8 hours, the solution was filtered. The residue was solvated in dry, distilled methanol. The resulting solution was dark red, and the solvent was removed in vacuo to yield a dark, red-colored solid (70 mg, 94.75 µmol). This complex was taken in a 1:1 methanol: ACN solution and used for crystallization via slow evaporation. Dark red crystals were obtained after a week. Yield: 60.81%

Analytical Calculation for C40H42ClCuN5O3(**2**) f_w=738.2272: (*expected*) C= 64.94, H= 5.72, N= 9.47; (*observed*) C= 64.47, H= 5.77, N= 9.39

UV-vis (in CH_3CN): λ, nm (ε, M^{-1} cm^{-1}): 427 nm (18324 M^{-1} cm^{-1}), 539 nm (23601 M^{-1} cm^{-1}), 563 nm (29783 M^{-1} cm^{-1})

HR-MS: 703.25 $[M]^+$

Scheme S1. Synthetic scheme for the **NDPA(H_3L)** ligand

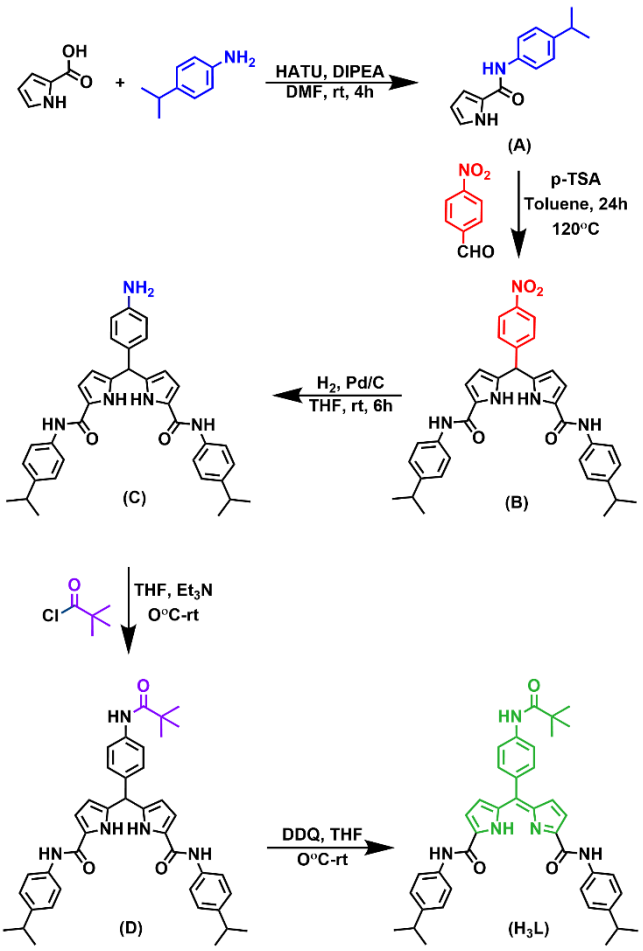

Scheme S2. Synthetic scheme for the **1**

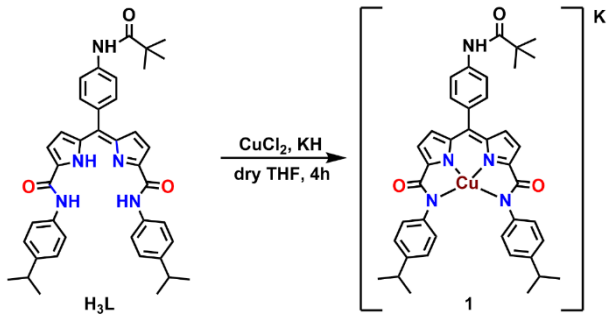

Scheme S3. Synthetic scheme for the **3**

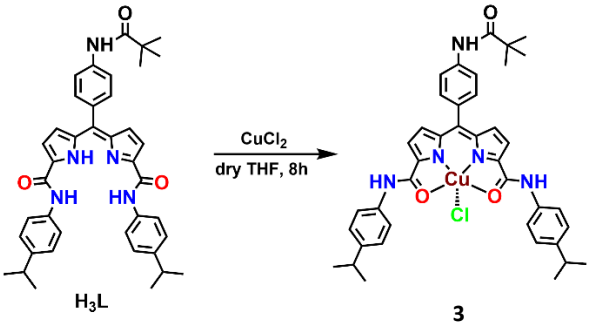

Characterization of synthesized ligand (NDPA):

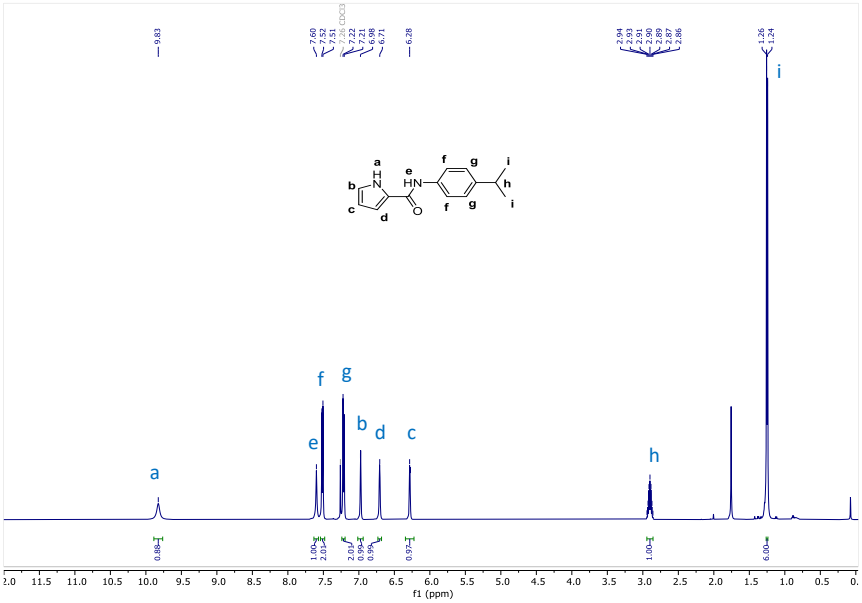

Figure S1: ^{1}H NMR of N-(4-isopropylphenyl)-1H-pyrrole-2-carboxamide (**A**) in $CDCl_3$

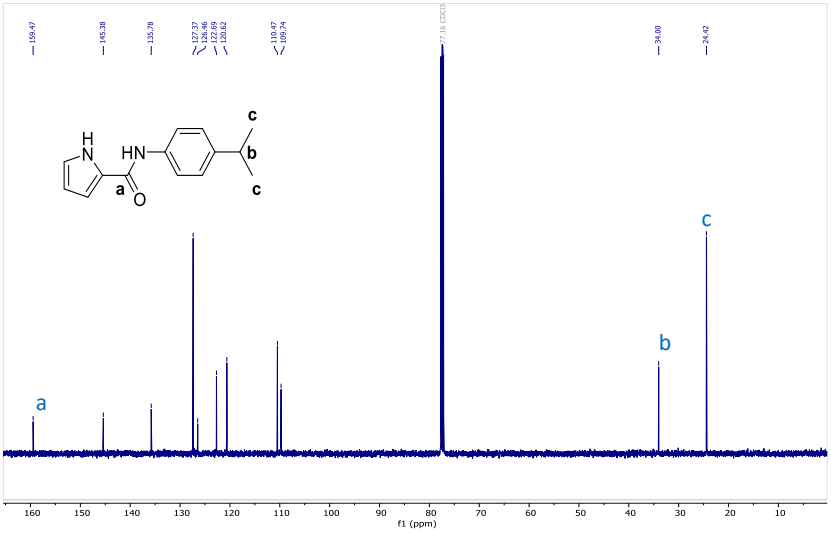

Figure S2: ^{13}C NMR of N-(4-isopropylphenyl)-1H-pyrrole-2-carboxamide (**A**) in $CDCl_3$

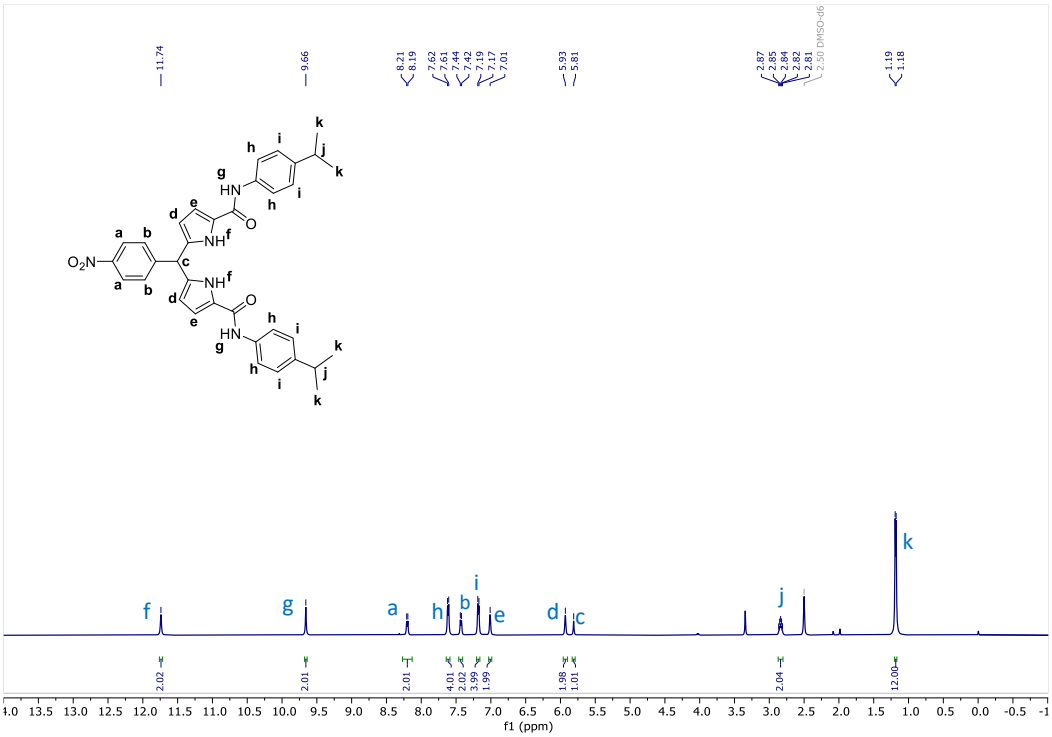

Figure S3: ^{1}H NMR of 5,5'-((4-nitrophenyl)methylene)bis(N-(4-isopropylphenyl)-1H-pyrrole-2-carboxamide) (**B**) in DMSO-d^{6}

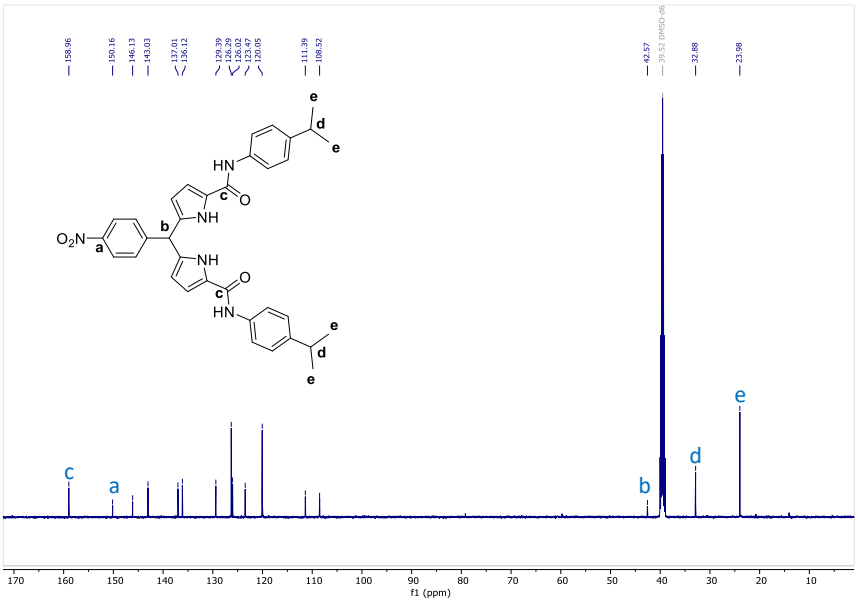

Figure S4: ^{13}C NMR of 5,5'-((4-nitrophenyl)methylene)bis(N-(4-isopropylphenyl)-1H-pyrrole-2-carboxamide) (**B**) in $CDCl_3$

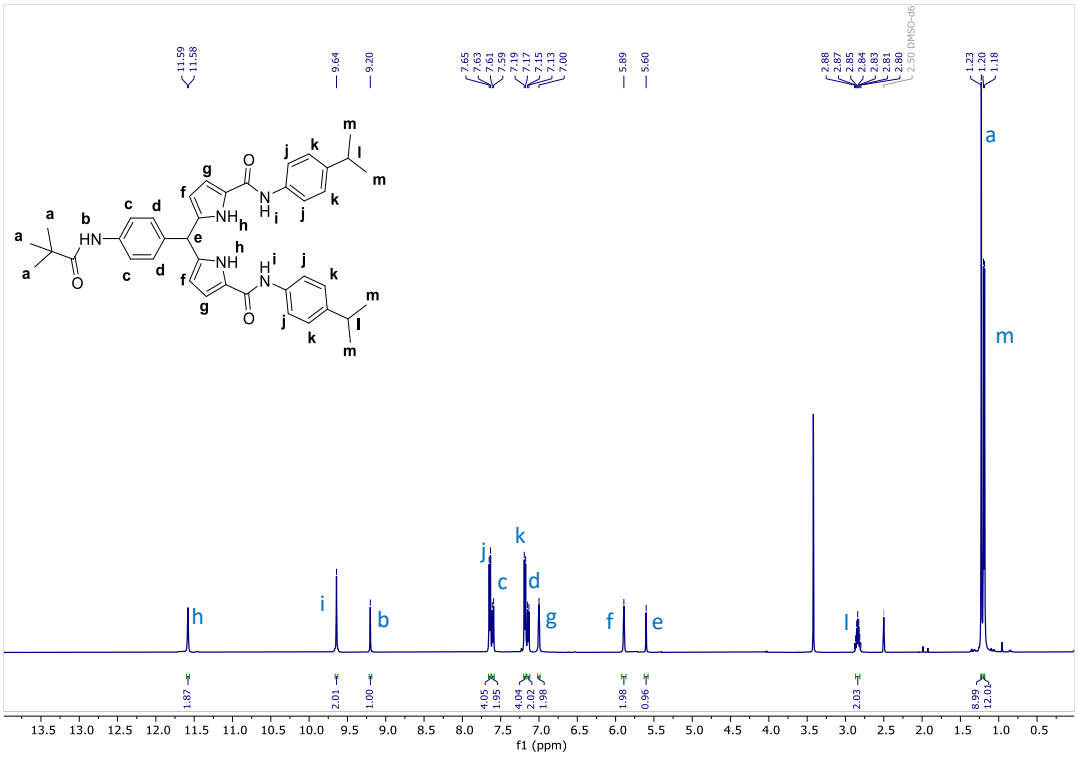

Figure S5: ^{1}H NMR of 5,5'-((4-pivalamidophenyl)methylene)bis(N-(4-isopropylphenyl)-1H-pyrrole-2-carboxamide) (**D**) in DMSO-d^{6}

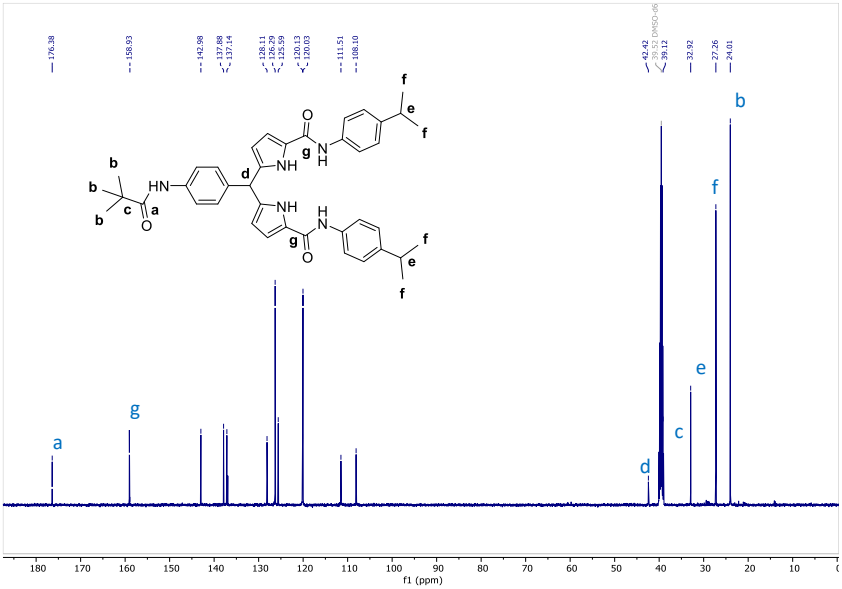

Figure S6: ^{13}C NMR of 5,5'-((4-pivalamidophenyl)methylene)bis(N-(4-isopropylphenyl)-1H-pyrrole-2-carboxamide) (**D**) in DMSO-d^{6}

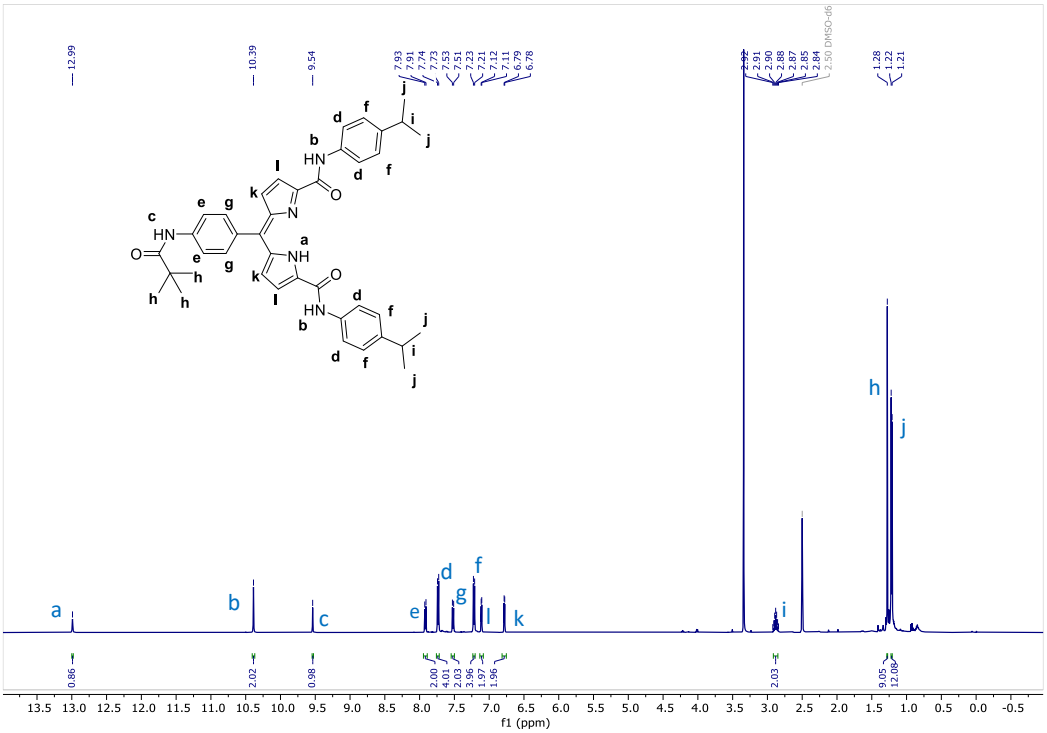

Figure S7: ^{1}H NMR of (Z)-N-(4-isopropylphenyl)-5-((5-((4-isopropylphenyl)carbamoyl)-2H-pyrrol-2-ylidene)(4-pivalamidophenyl)methyl)-1H-pyrrole-2-carboxamide (**H_3L**) in DMSO-d^{6}

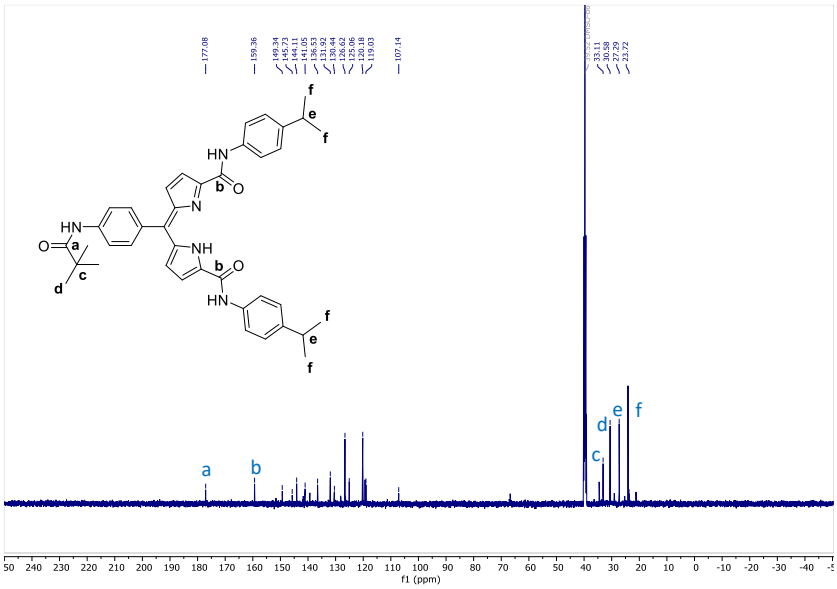

Figure S8: ^{13}C NMR of (Z)-N-(4-isopropylphenyl)-5-((5-((4-isopropylphenyl)carbamoyl)-2H-pyrrol-2-ylidene)(4-pivalamidophenyl)methyl)-1H-pyrrole-2-carboxamide (**H_3L**) in DMSO-d^{6}

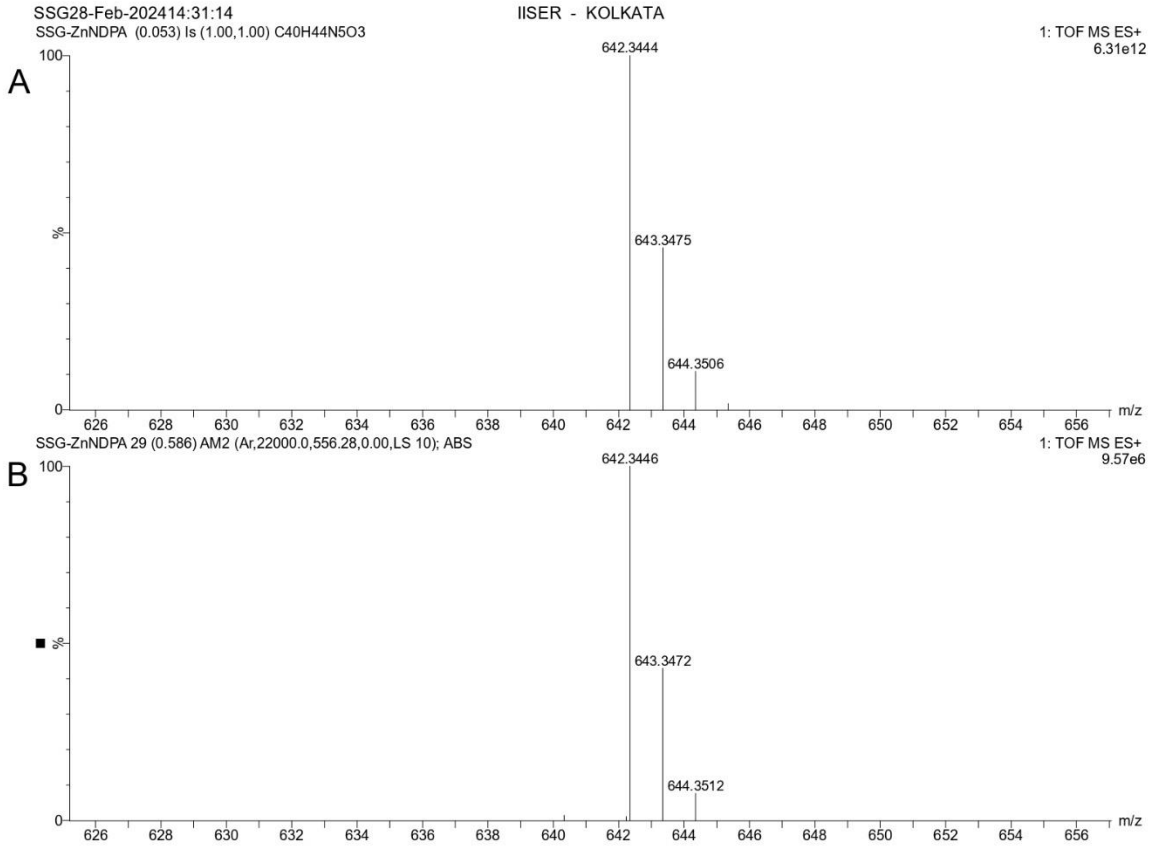

Figure S9: HR-MS for compound (Z)-N-(4-isopropylphenyl)-5-((5-((4-isopropylphenyl)carbamoyl)-2H-pyrrol-2-ylidene)(4-pivalamidophenyl)methyl)-1H-pyrrole-2-carboxamide (**H_3L**) in Methanol (m/z: **641.3366**) – (A) Simulated mass: **642.3444** $[M + H]^+$, (B) Experimental mass: **642.3446** $[M + H]^+$

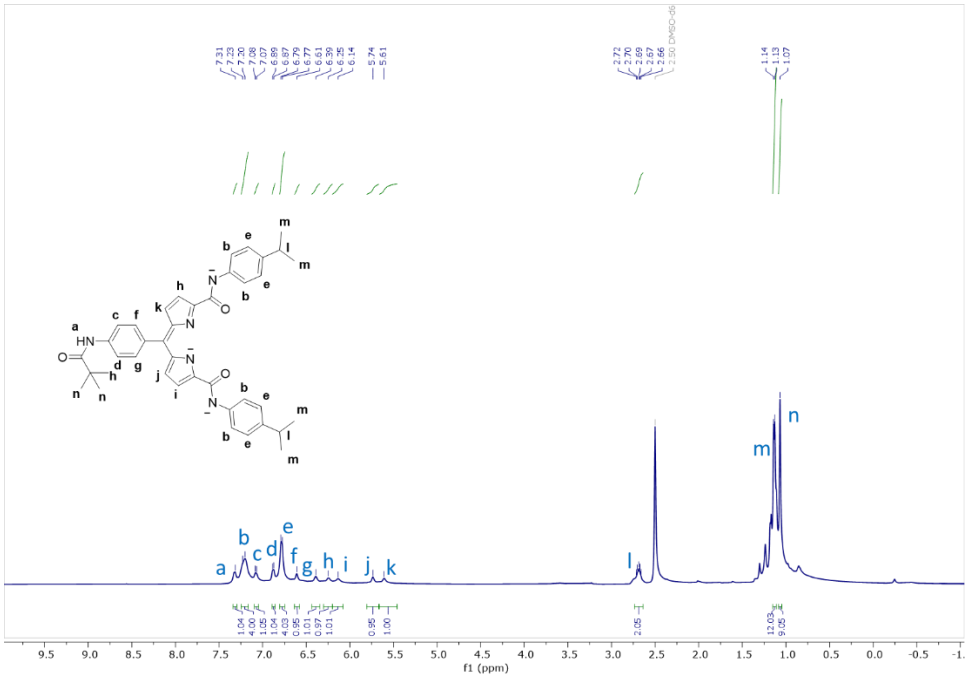

Figure S10: ^1H NMR of L^{3-} in DMSO-d^6

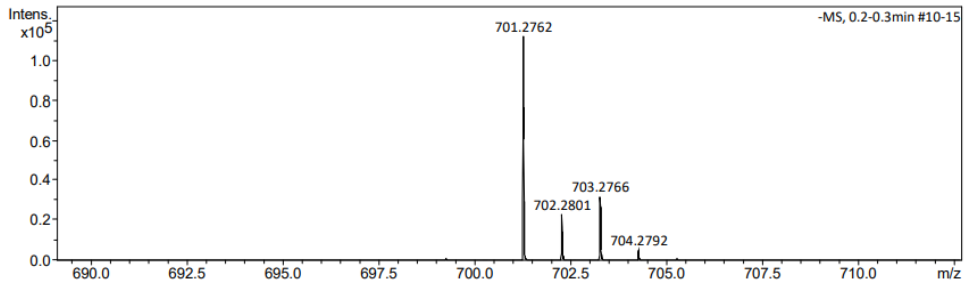

Figure S11: HR-MS spectra in negative ion mode for metal complex K[Cu(NDPA)](**1**) in Acetonitrile (m/z **701.24**) **701.27** [M]$^-$

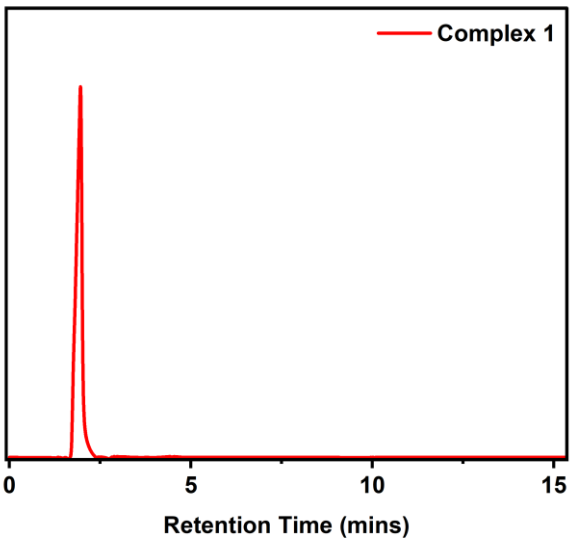

Figure S12: HPLC spectra of **1**

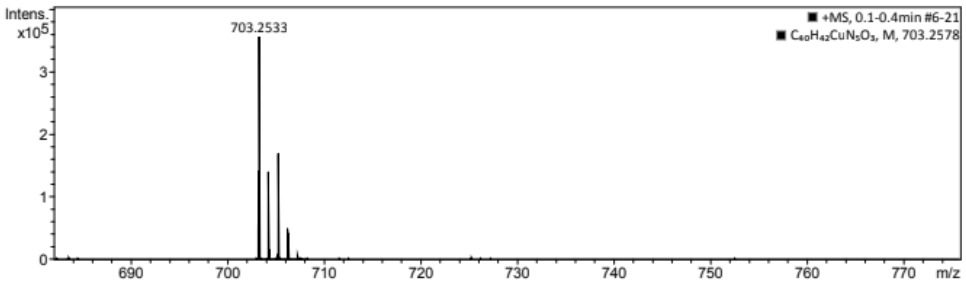

Figure S13: HR-MS spectra in positive ion mode for metal complex [Cu(NDPA)Cl] showing N_2O_2 coordination (**3**) in Acetonitrile (m/z **703.2585**) **703.2533** [M]$^+$

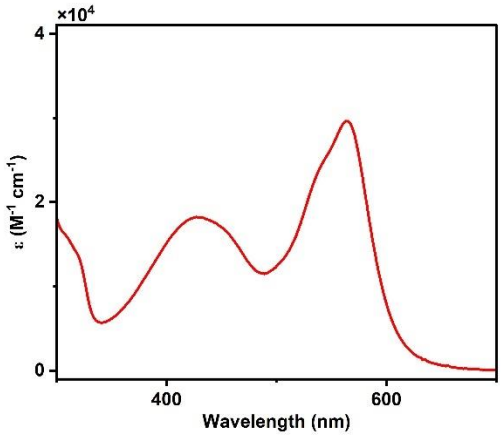

Figure S14: UV-vis absorption spectra of Complex **3** in acetonitrile.

SC-XRD structural analysis of $[K^+(18\text{-crown-6})][Cu(NDPA)]$ with N_4 coordination (Complex 1):

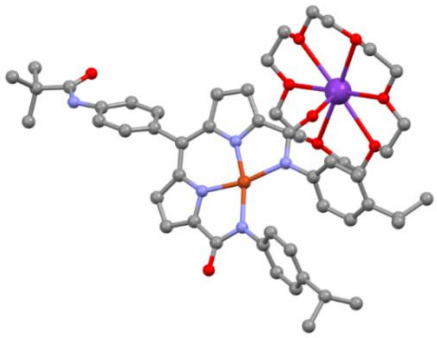

Figure S15: SC-XRD structure for **$[K^+(18\text{-crown-6})][Cu(NDPA)]$**

CCDC Number	2313077
Identification code	(18-C-6)K[Cu(NDPA)]
Empirical formula	$C_{54}H_{67}CuKN_6O_9$
Formula weight	1046.77
Crystal Colour	Dark Violet
Temperature/K	100.00(2)
Crystal system	triclinic
Space group	P-1
a/Å	9.0901(2)
b/Å	13.3962(2)
c/Å	22.3177(3)
α/°	77.1960(10)
β/°	86.4310(10)
γ/°	82.8870(10)
Volume/Å^3	2628.01(8)
Z	2
ρ_{calc}g/cm^3	1.323
μ/mm^{-1}	1.792
F(000)	1106.0
Crystal size/mm^3	0.08 × 0.04 × 0.02

Radiation	Cu Kα (λ = 1.54184)
Index ranges	-10 ≤ h ≤ 10, -16 ≤ k ≤ 13, -26 ≤ l ≤ 26
Reflections collected	9566
Independent reflections	8628 [R_{int} = 0.0777, R_{sigma} = 0.0350]
Data/restraints/parameters	9166/0/648
Goodness-of-fit on F^2	1.073
Final R indexes [I>=2σ (I)] [a,b]	R_1 = 0.0373 [a], wR_2 = 0.1010 [b]
Final R indexes [all data] [a,b]	R_1 = 0.0409 [a], wR_2 = 0.1038 [b]

[a] $R_1 = \Sigma||F_o| - |F_c||/\Sigma|F_o|$. [b] $wR_2 = \{\Sigma[w\,(|F_o|^2 - |F_c|^2)^2\,]/\Sigma[w(|F_o|^2)^2]\}^{1/2}$.

Table S1: Crystal Data and Data Collection Parameters for K[Cu(NDPA)](**1**)

Table for Bond Lengths (Å)		
Atom	**Atom**	**Length/Å**
Cu1	N1	1.9442(14)
Cu1	N3	1.9355(14)
Cu1	N4	2.0141(14)
Cu1	N5	1.9981(14)

Table S2: Cu-N bond length parameters of (**1**)

Table for Bond Angles (˚)			
Atom	**Atom**	**Atom**	**Angle/˚**
N4	Cu1	N1	164.92(6)
N3	Cu1	N5	166.14(6)
N3	Cu1	N1	84.20(6)
N3	Cu1	N4	81.29(6)
N4	Cu1	N5	112.48(6)
N5	Cu1	N1	81.95(6)

Table S3: N-Cu-N bond angle parameters of Complex (**1)**

Table for Bond Lengths (Å)		
Atom	**Atom**	**Length/Å**
C23	N4	1.419(2)
C22	N4	1.356(2)
C22	O3	1.250(2)
C21	C22	1.489(14)
C21	N3	1.329(2)
C21	C20	1.416(2)
C20	C19	1.378(2)
C19	C18	1.427(2)
C18	C6	1.409(2)
C6	C5	1.407(2)
C5	C4	1.427(2)
C4	C3	1.380(2)
C3	C2	1.422(2)
C2	N1	1.328(2)
C5	N1	1.384(2)
C2	C1	1.485(2)
C1	O1	1.242(2)
C1	N5	1.361(2)
C32	N5	1.417(2)

Table S4: Table for Bond Lengths (Å) of (**1**)

SC-XRD structural analysis of [Cu(NDPA)Cl] with N_2O_2 coordination (Complex 3):

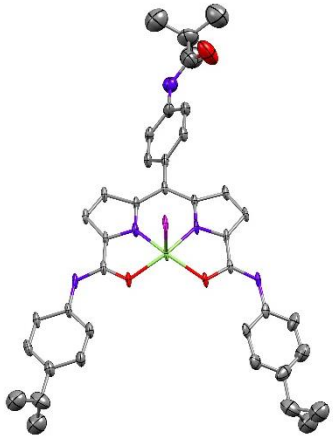

Figure S16: SC-XRD structure of **[Cu(NDPA)Cl]** with N_2O_2 coordination (Complex 3)

CCDC Number	2370489
Identification code	CuNDPA-Cl_N_2O_2
Empirical formula	$C_{40}H_{48}ClCuN_7O_3$
Formula weight	821.88
Crystal Colour	Dark Red
Temperature/K	100.15(2)
Crystal system	triclinic
Space group	P-1
a/Å	9.6787(3)
b/Å	10.7885(4)
c/Å	20.4415(8)
α/°	96.743(3)
β/°	90.805(3)
γ/°	99.865(3)
Volume/Å^3	2087.09(13)
Z	2
ρ_{calc}g/cm^3	1.308
μ/mm^{-1}	1.708

F(000)	862.0
Crystal size/mm^3	0.4 × 0.3 × 0.2
Radiation	Cu Kα (λ = 1.54184)
Index ranges	-11 ≤ h ≤ 11, -10 ≤ k ≤ 12, -24 ≤ l ≤ 24
Reflections collected	40872
Independent reflections	7376 [R_{int} = 0.0643, R_{sigma} = 0.0397]
Data/restraints/parameters	7376/116/431
Goodness-of-fit on F^2	1.400
Final R indexes [I>=2σ (I)] [a,b]	R_1 = 0.1256 [a], wR_2 = 0.3404 [b]
Final R indexes [all data] [a,b]	R_1 = 0.1406 [a], wR_2 = 0.3535 [b]

[a] $R_1 = \Sigma||F_o| - |F_c||/\Sigma|F_o|$. [b] $wR_2 = \{\Sigma[w\,(|F_o|^2 - |F_c|^2)^2\,]/\Sigma[w(|F_o|^2)^2]\}^{1/2}$

Table S5: Crystal Data and Data Collection Parameters for **[Cu(NDPA)Cl]**(**3**)

Table for Bond Lengths (Å)		
Atom	**Atom**	**Length/Å**
Cu1	N1	1.893(5)
Cu1	N3	1.913(5)
Cu1	O1	2.045(4)
Cu1	O3	2.014(4)
Cu1	Cl1	2.5876(16)

Table S6: Cu-N, Cu-O, and Cu-Cl bond length parameters of (**3**)

Table for Bond Angles (˚)			
Atom	**Atom**	**Atom**	**Angle/˚**
O1	Cu1	Cl1	97.48(12)
O3	Cu1	O5	107.53(17)
O3	Cu1	Cl1	93.85(12)
N3	Cu1	O1	159.99(18)
N3	Cu1	O3	81.77(19)
N3	Cu1	Cl1	99.55(15)

N1	Cu1	O1	81.81(19)
N1	Cu1	O3	165.85(18)
N1	Cu1	N3	86.2(2)
N1	Cu1	Cl1	91.44(14)

Table S7: N-Cu-N bond angle parameters of Complex (**3)**

Table for Bond Lengths (Å)		
Atom	**Atom**	**Length/Å**
C23	N4	1.396(9)
C22	N4	1.348(7)
C22	O3	1.263 (7)
C21	C22	1.464(9)
C21	N3	1.340(7)
C21	C20	1.418(9)
C20	C19	1.353(9)
C19	C18	1.435(7)
C18	C6	1.429(8)
C6	C5	1.445(8)
C5	C4	1.433(7)
C4	C3	1.372(9)
C3	C2	1.425(8)
C2	N1	1.340(7)
C5	N1	1.345(8)
C2	C1	1.441(9)
C1	O1	1.280(6)
C1	N5	1.331(7)
C32	N5	1.405(7)

Table S8: Table for Bond Lengths (Å) of Complex **3**

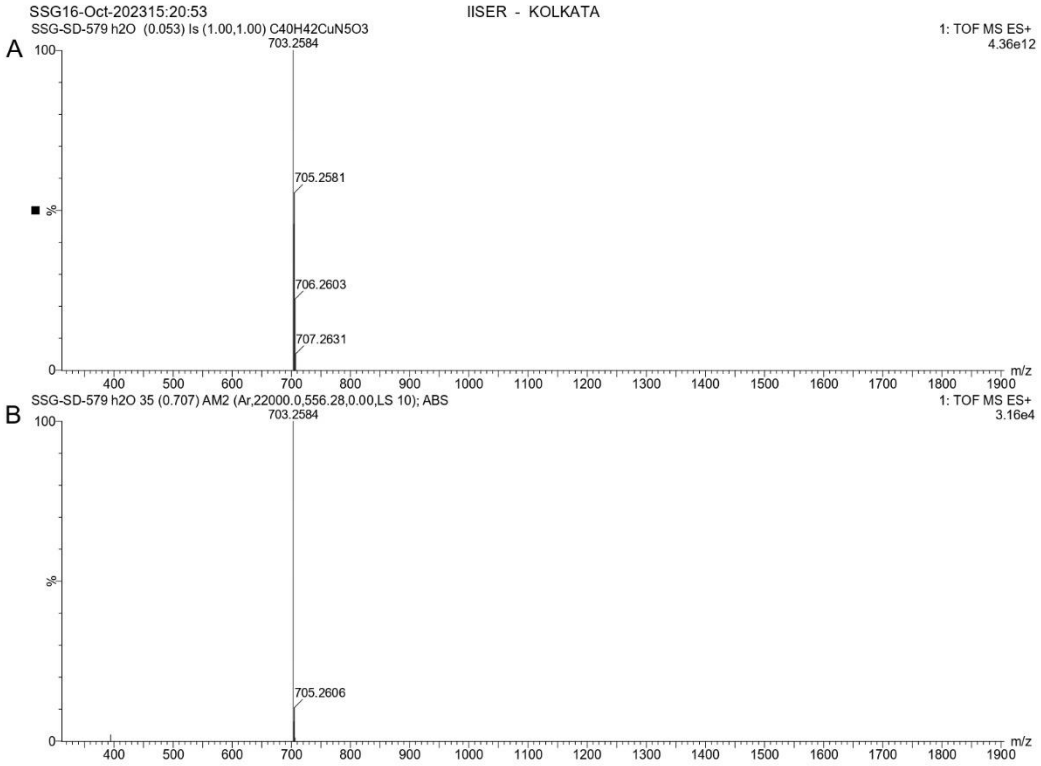

Figure S17: HR-MS spectra of **2** (m/z: **702.2505**) in positive ion mode after the addition of H_2O in the acetonitrile solution of **1** – (A) Simulated mass: **703.2584** $[M + H]^+$, (B) Experimental mass: **703.2584** $[M+ H]^+$

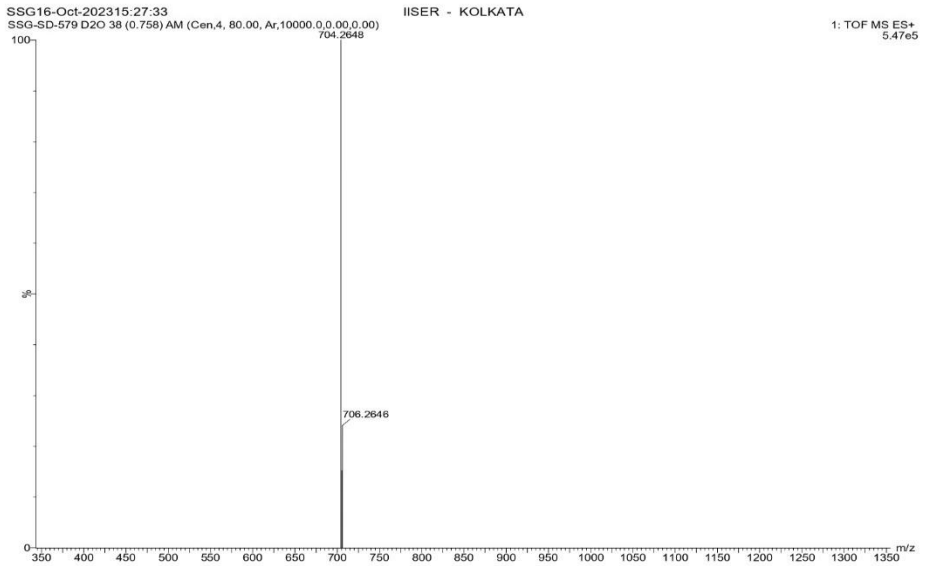

Figure S18: HR-MS spectra of **2** in positive ion mode after the addition of D_2O in the acetonitrile solution of **1** (expected m/z: **704.2646**, observed m/z: **704.2648**)

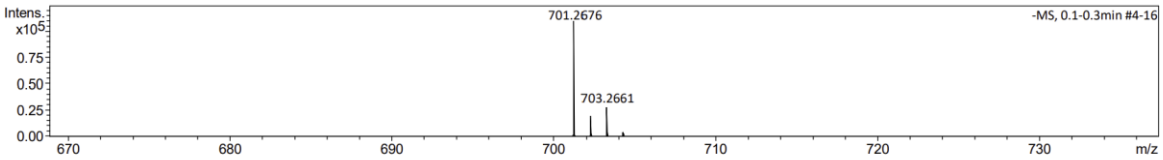

Figure S19: HR-MS spectra of **2** in negative ion mode after the addition of Et_3N in the acetonitrile solution **701.2676** [M^-]

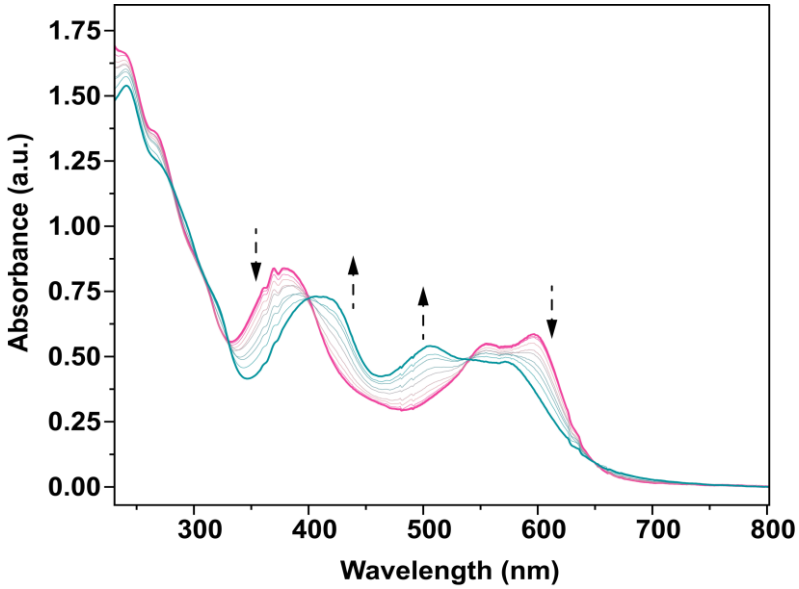

Figure S20: Absorption spectral change due to the coordination change from N_4(**1**), pink spectrum, to N_3O(**2**), blue spectrum, with the addition of 13μM water per addition/scan; overall 0.117mM water was added for this conversion

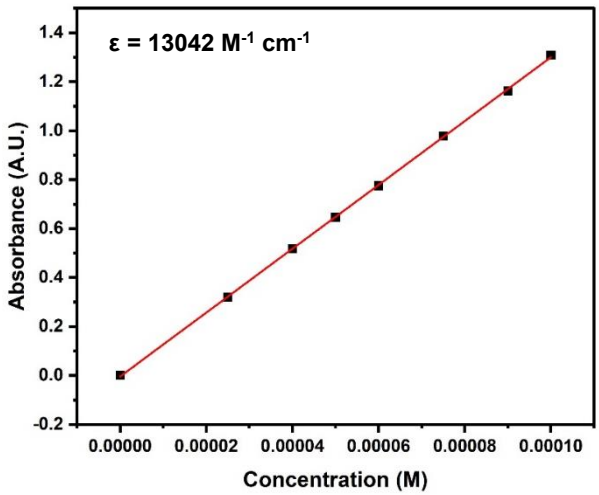

Figure S21: Molar absorption coefficient ($M^{-1}cm^{-1}$) of **1** for 378 nm peak

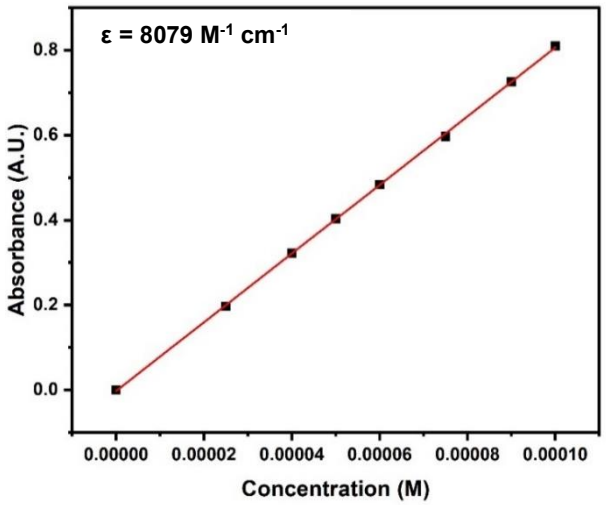

Figure S22: Molar absorption coefficient ($M^{-1}cm^{-1}$) of **1** for 556 nm peak

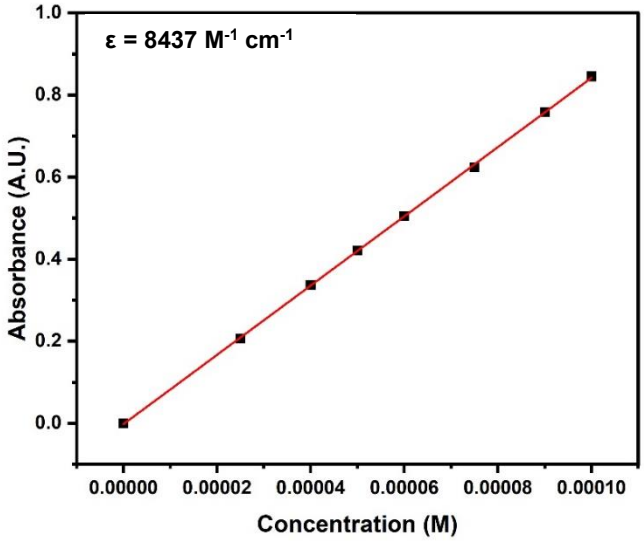

Figure S23: Molar absorption coefficient ($M^{-1}cm^{-1}$) of **1** for 598 nm peak

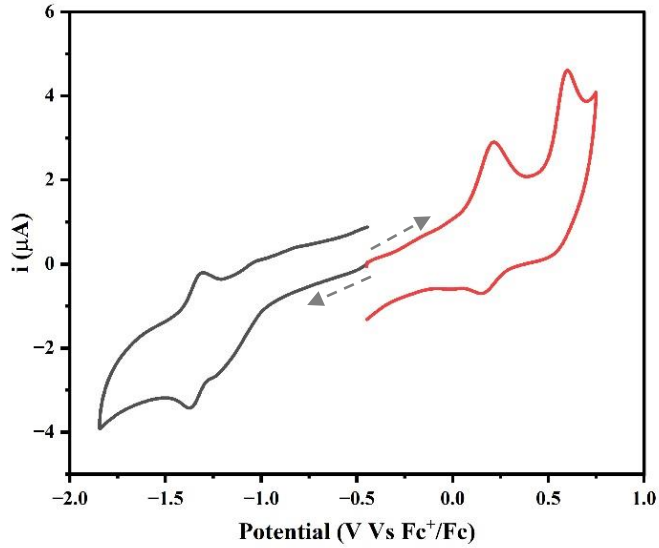

Figure S24: Cyclic voltammogram of 0.5 mM **1** in Ar-saturated acetonitrile with 0.1 M $TBAPF_6$. WE: GC, RE: Ag/AgCl, CE: Pt wire, Scan rate: 100 mV s^{-1}

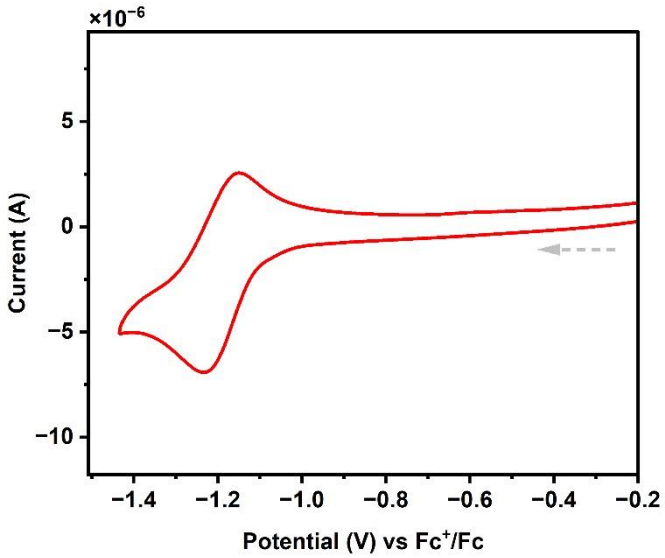

Figure S25: Cyclic voltammogram of **H_3L** in Ar-saturated acetonitrile with 0.1 M $TBAPF_6$. WE: GC, RE: Ag/AgCl, CE: Pt wire, Scan rate: 100 mV s^{-1}

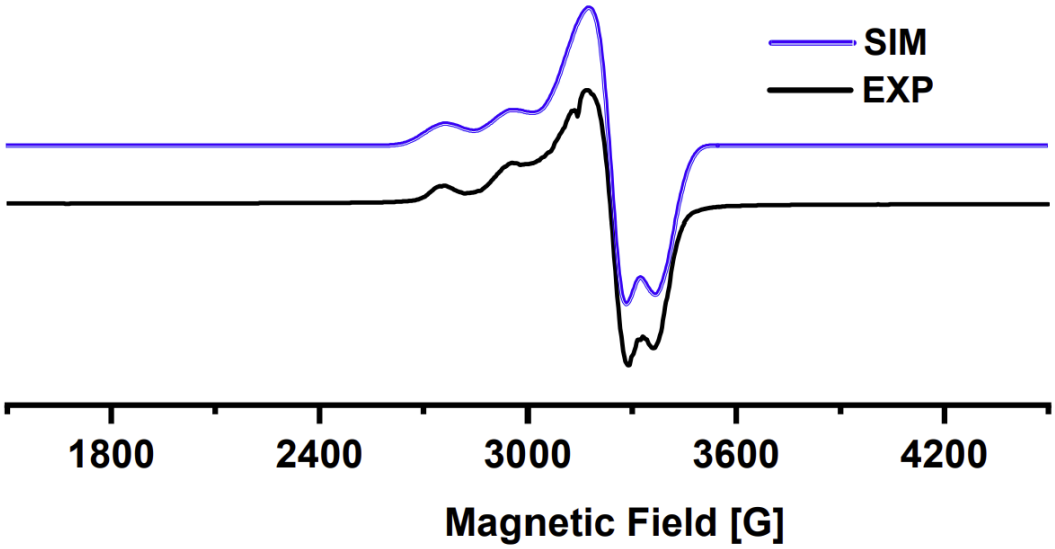

Figure S26: X-band EPR spectrum (v = 9.300 GHz, power = 1.65 mW, receiver gain = 1 x 10^6, modulation frequency = 100 KHz, modulation amplitude = 10.00 G) recorded for 1 mM solution of **1** in acetonitrile: Toluene (3:1) at 90 K. The N superhyperfine splitting in the spectrum was also observed. only Cu-based (I = 3/2) splitting was observed with corresponding g-values of $g_{\perp}$ = 2.050 and $g_{\parallel}$ = 2.167. The simulation-derived hyperfine coupling constant parameters are as follows: $A^{Cu}_{(xx)}$ = 10 x 10^{-4} cm^{-1}, $A^{Cu}_{(zz)}$ = 190 x 10^{-4} cm^{-1}, $A^{4N}_{(xx)}$ = 10 x 10^{-4} cm^{-1}, $A^{4N}_{(yy)}$ = 30 x 10^{-4} cm^{-1}

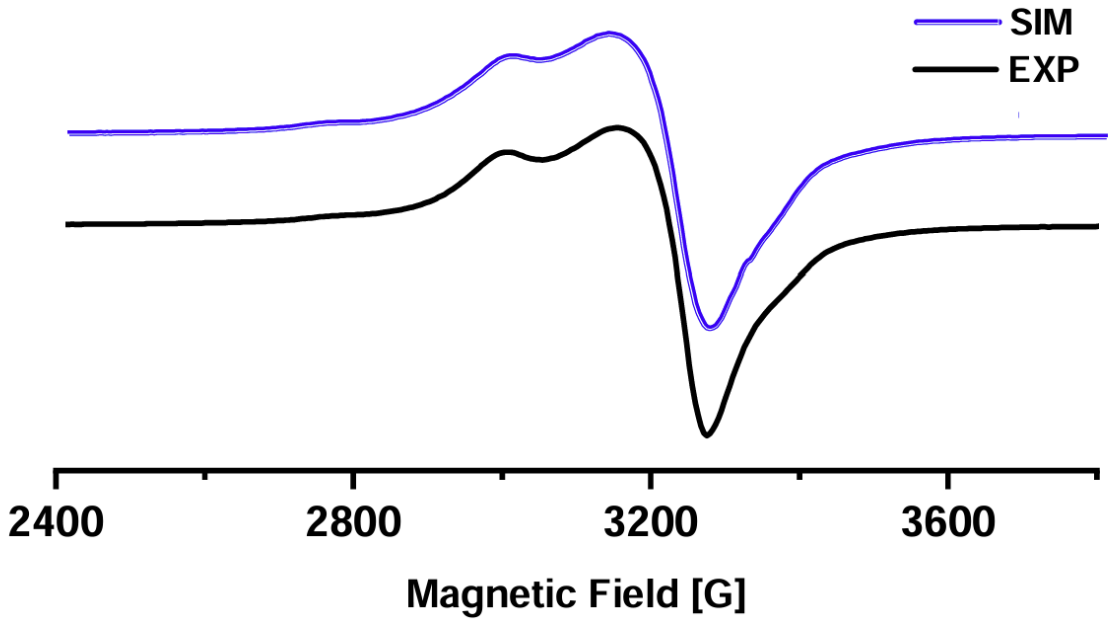

Figure S27: X-band EPR spectrum (v = 9.300 GHz, power = 1.65 mW, receiver gain = 1 x 10^6, modulation frequency = 100 KHz, modulation amplitude = 10.00 G) recorded for 1 mM solution of **2** in acetonitrile: Toluene (3:1) at 90 K. No N hyperfine was noted; only Cu-based (I = 3/2) splitting was observed with corresponding g-values of $g_{\perp}$ = 2.052 and $g_{\parallel}$ = 2.271. The simulation-derived hyperfine coupling constant parameters are as follows: $A^{Cu}_{(xx)}$ = 5 x 10^{-4} cm^{-1}, $A^{Cu}_{(yy)}$ = 20 x 10^{-4} cm^{-1}, $A^{Cu}_{(zz)}$ = 110 x 10^{-4} cm^{-1}.

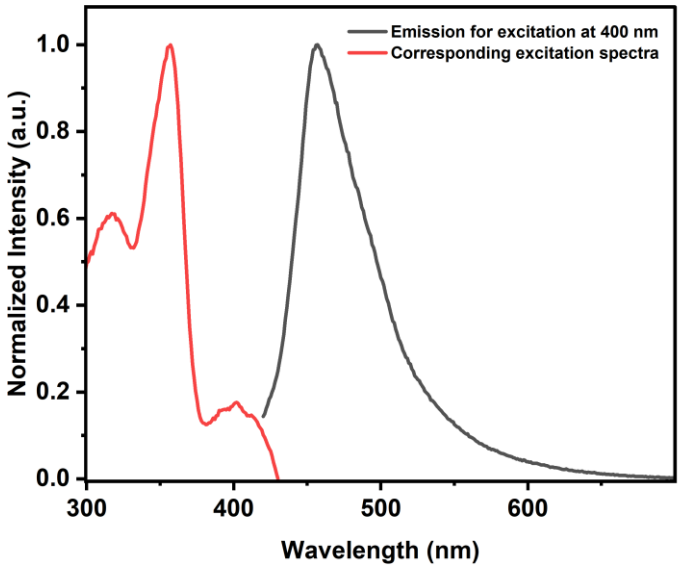

Figure S28: Normalized emission (excitation wavelength: 400 nm) spectra of **H_3L** in acetonitrile

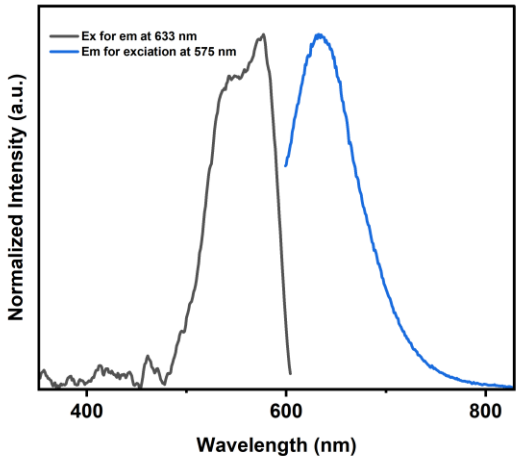

Figure S29: Normalized emission (excitation wavelength: 575 nm) spectra of **1** in acetonitrile

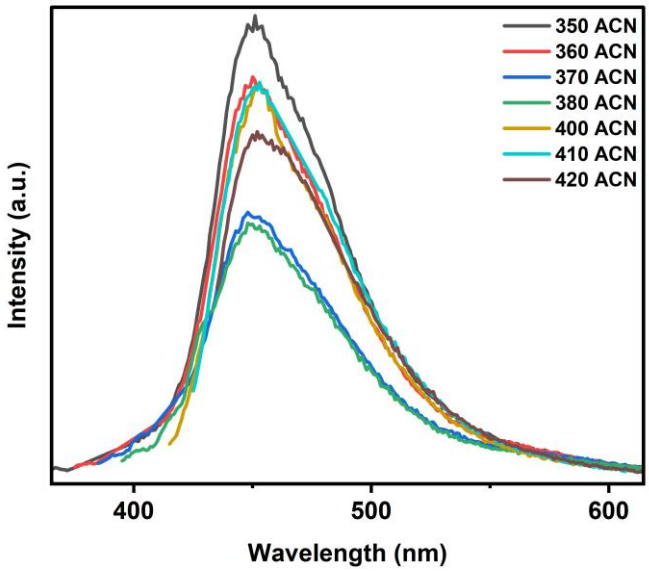

Figure S30: Emission spectra of **1** in acetonitrile for different excitation wavelength 350nm-420nm

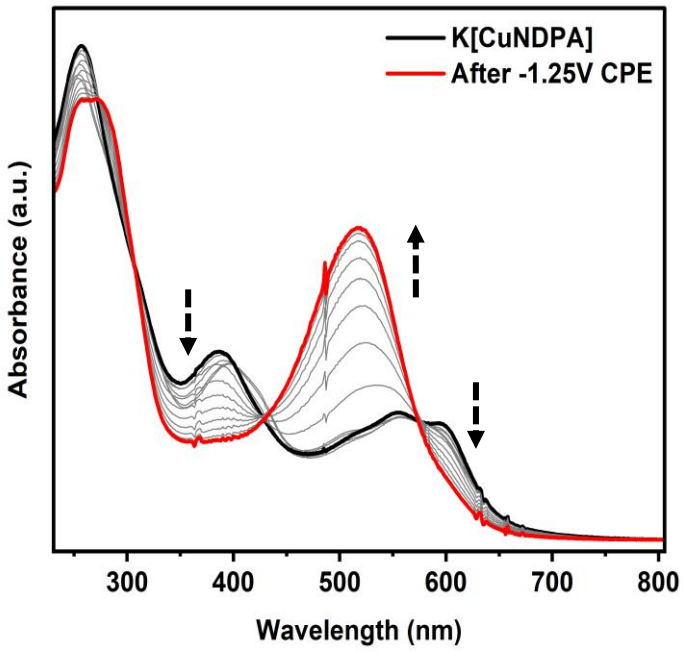

Figure S31: Absorption spectral change after CPE at -1.25V (Fc^{+}/Fc)

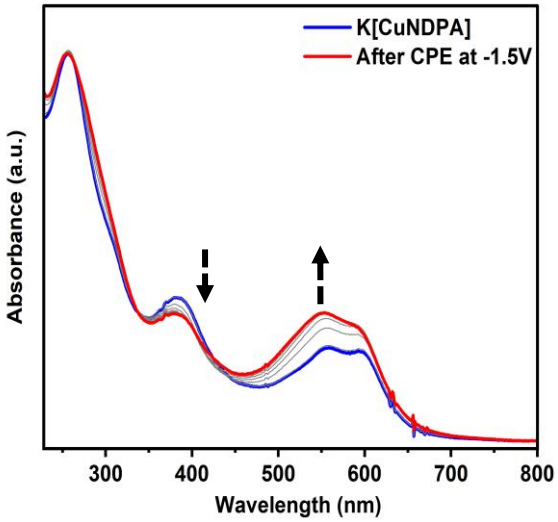

Figure S32: Absorption spectral change after CPE at -1.5V (Fc^+/Fc)

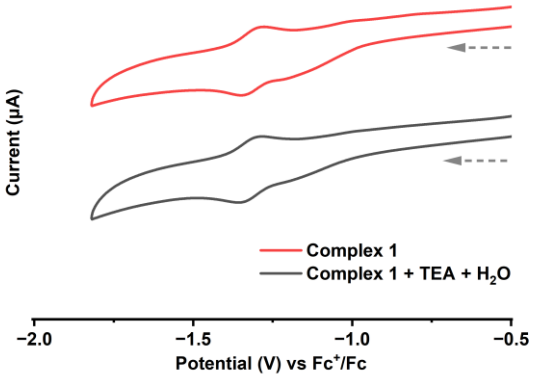

Figure S33: Cyclic voltammogram of 0.5 mM **1** in the presence of 70 mM Et_3N and 5% water in Ar-saturated acetonitrile with 0.1 M $TBAPF_6$. WE: GC, RE: Ag/AgCl, CE: Pt wire, Scan rate: 100 mV s^{-1}

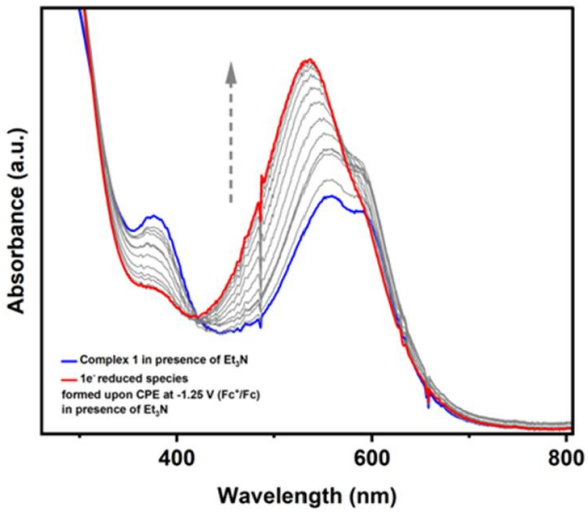

Figure S34: Absorption spectral change after CPE at -1.25V (Fc^+/Fc) of Complex **1** in the presence of 70 mM Et_3N and 5% water

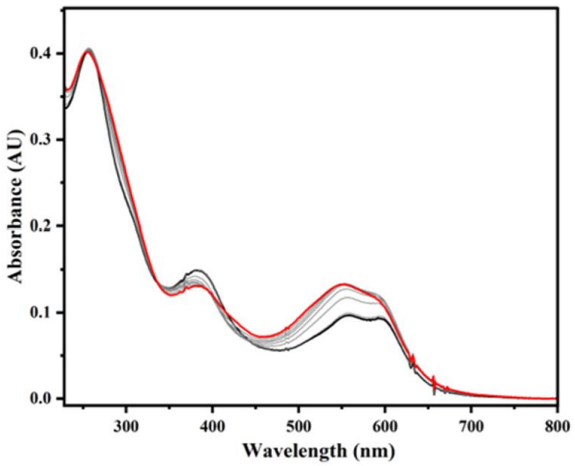

Figure S35: Absorption spectral change after CPE at -1.5V (Fc^+/Fc) of Complex **1** in the presence of 70 mM Et3N and 5% water

Calculation on excited state potential:

It would be noteworthy to calculate the excited state redox potential from the electrochemical potential and $E_{0\text{-}0}$. Thus, the intersection of normalized absorption and emission spectra leads to excited energy of ^{2}LMCT state, $E_{0\text{-}0}$ =2.88 eV = 23228.95 cm^{-1}.(Isr. J. Chem. **1970,** 8 (2), 259-271) These results in the excited state redox potential of $^1E_{ox}^*$ = -2.70 V *vs* Fc^+/Fc, $^2E_{ox}^*$ = -2.31 V *vs* Fc^+/Fc , and $^1E_{red}^*$ = 1.76 V *vs* Fc^+/Fc, $^2E_{red}^*$ = 1.50 V *vs* Fc^+/Fc .

Entry	1 (μM)	[TEA] (mM)	[H_2O] (% v/v)	Irradiation Time (h)	CO (μmol)	H_2 (μmol)	TON_{CO}	TOF_{CO}^{max} (h^{-1})	TON_{H2}	Selectivity for CO (%)
1	100	70	0	2	76.8	2.5	256	128	8	97 : 3
2	100	70	0.5	2	102.5	2.6	342	171	8	98 : 2
3	100	70	1	2	129.3	2.2	431	216	7	98 : 2
4	100	70	1.5	2	170.9	2.9	570	285	10	98 : 2
5	100	70	2	2	209.5	2.9	698	349	10	99 : 1
6	100	70	3	2	237.3	3.2	791	395	10	99 : 1
7	100	70	4	2	290.5	3.1	968	484	10	99 : 1
8	100	70	5	2	339.7	2.2	1132	566	7	99 : 1
9	100	70	10	2	229.7	2.9	766	383	10	99 : 1

Table S9: Photocatalytic reduction of CO_2 to CO upon irradiation for 2 hrs of a CO_2-saturated acetonitrile solution containing 100μM of **1**, 70 mM Et_3N and varying amounts of H_2O (in % v/v) upon irradiation by 390 nm light

Entry	1 (μM)	[TEA] (mM)	[H_2O] (%)	Irradiation Time (h)	CO (μmol)	H_2 (μmol)	TON_{CO}	TOF_{CO}^{max} (h^{-1})	TON_{H2}	Selectivity for CO (%)
1	100	25	5	2	278.4	2.4	921	461	8	99 : 1
2	100	50	5	2	305.0	2.7	1017	508	9	99 : 1
3	100	70	5	2	339.7	2.2	1132	566	7	99 : 1
4	100	95	5	2	279.5	3.0	932	466	10	99 : 1
5	100	120	5	2	268.8	3.7	896	448	12	99 : 1

Table S10: Photocatalytic CO2 reduction to CO upon irradiation for 2 hrs of a CO2-saturated acetonitrile solution containing 100μM of **1**, varying amounts of Et_3N and 5% H_2O (v/v) in 390 nm light

Light used	1 (μM)	[TEA] (mM)	[H_2O] (%)	Irradiation Time (h)	CO (μmol)	H_2 (μmol)	TON_{CO}	TOF_{CO}^{max} (h^{-1})	TON_{H2}	Selectivity for CO (%)
390 nm	100	70	5	2	339.7	2.2	1132	566	7	99 : 1
Solar Simulator (Xe lamp) 400-750nm	100	70	5	2	278.6	2.2	929	465	7	99 : 1
426 nm	100	70	5	2	144.6	2.3	482	241	8	98 : 2
Sunlight	100	70	5	4	275.9	1.7	920	230	5	99:1

Table S11: Photocatalytic CO_2 reduction to CO upon irradiation of a CO_2-saturated acetonitrile solution containing 100μM of **1** in different visible light sources.

Control Condition	1 (μM)	[TEA] (mM)	[H_2O] (%)	Irradiation Time (h)	CO (μmol)
Dark	100	25	5	2	0
Ar atmosphere	100	50	5	2	0

Table S12: Control reactions containing 100μM of **1** in different visible light sources.

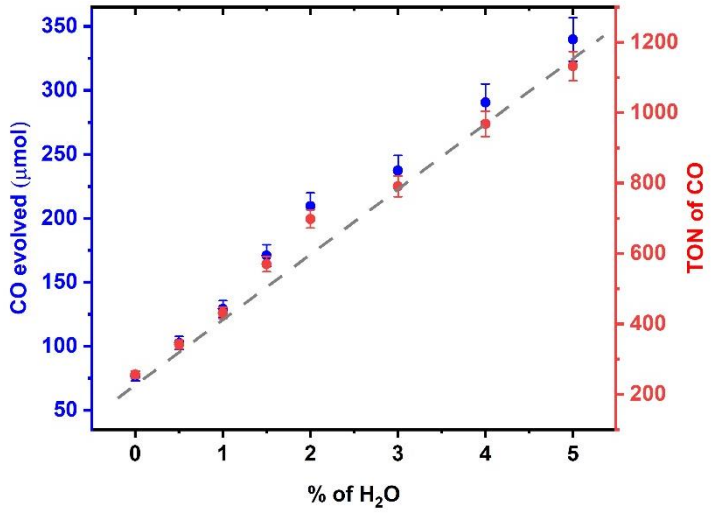

Figure S36: Photocatalytic CO_2 reduction [TON (red) and amounts (blue)] to CO irradiated for 2 hrs in CO_2-saturated acetonitrile solution containing 100μM of **1**, 70 mM Et_3N and varying amounts of H_2O (in %v/v)

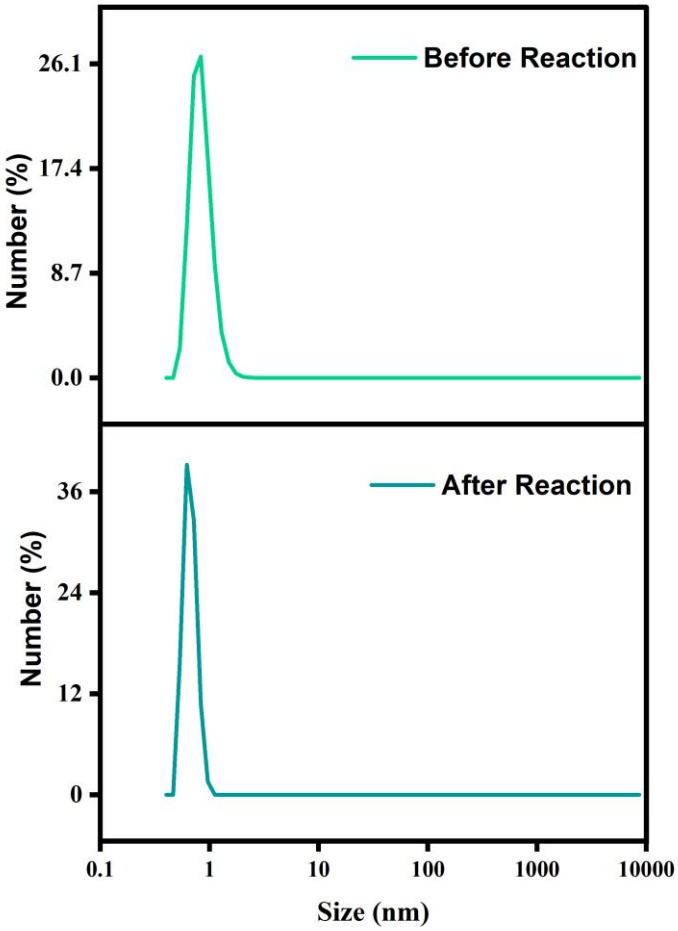

Figure S37: Particle size distribution of a CO_2-saturated acetonitrile solution containing 0.1 mM **1**, 70 mM of TEA, and 1% H_2O before and after irradiation in DLS

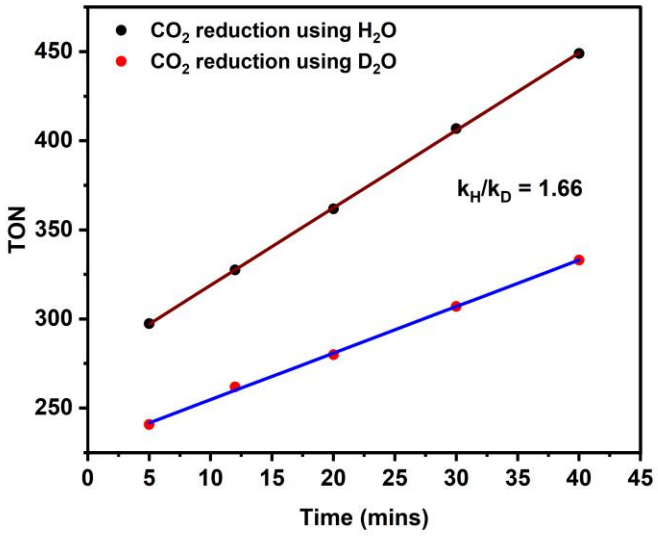

Figure S38: Plots of TON versus time determined in presence of H_2O (Red line) and D_2O (Blue line)

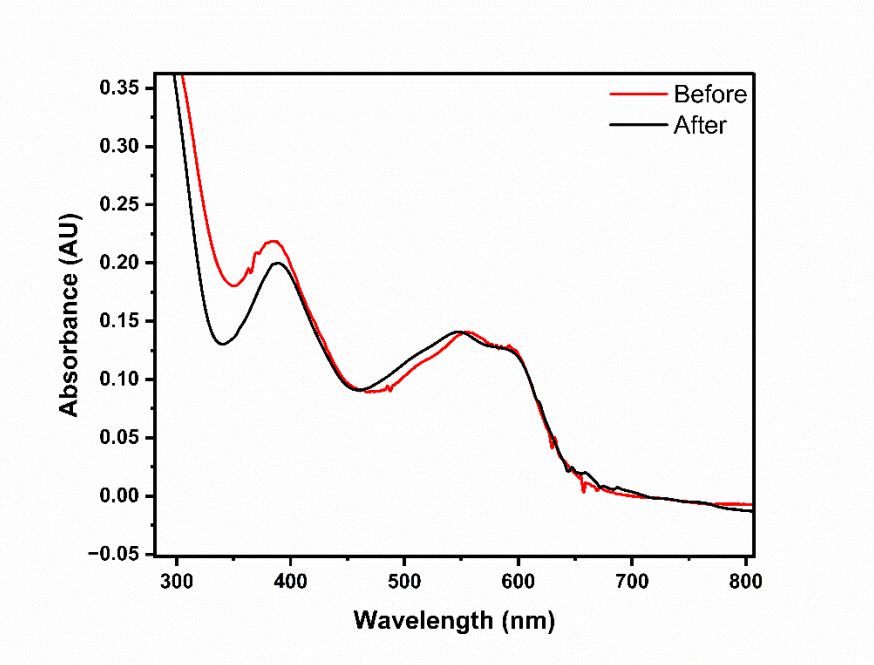

Figure S39: UV-vis absorption spectra of **1** in acetonitrile (Red line) and of the reaction mixture after photocatalysis for 2h in the presence of CO_2 (Black line)

Photobleaching Control :

Fluorescence intensity was measured after irradiation with 390nm (light used for photocatalysis) light for 10 min, and this measurement was repeated two times. No change in intensity was observed with the initial fluorescence peak. In the case of photobleaching, demetallation can increase the fluorescent intensity.

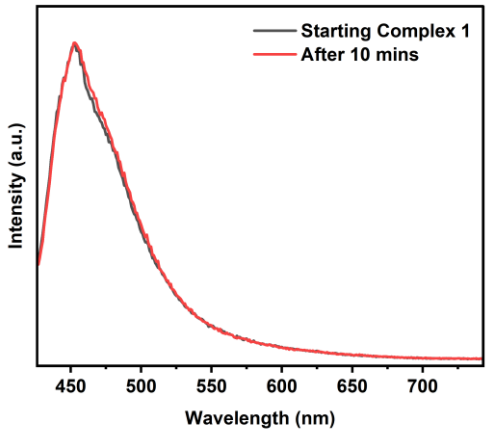

Figure S40: Emission spectra (ex. 400nm) of **1** before and after 10 min irradiation under 390nm light in acetonitrile

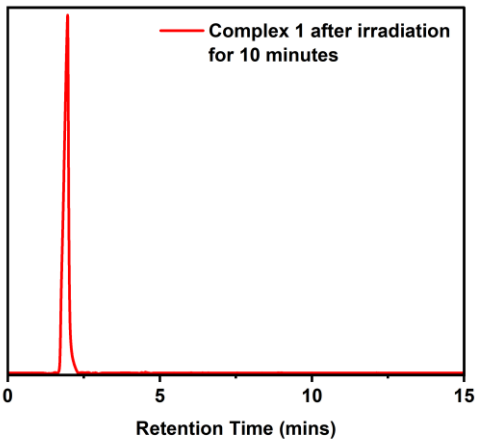

Figure S41: HPLC spectra of **1** after 10 min irradiation under 390nm light in acetonitrile

Average Lifetime:

Excited state lifetime for multi-exponent decays is always reported using the averaged lifetime (τ_{avg}) calculated as shown below:

$$< \tau_{avg} > = \frac{\Sigma_i A_i \tau_i^2}{\Sigma_i A_i \tau_i}$$

where A_i stands for the corresponding amplitude of each component and τ_i stands for the excited state lifetime of that component's decay curve.

Complex	τ_1 (ns)	τ_2(ns)	τ_{avg}(ns)	χ^2
Complex **1**	0.3 (18.99)	4.29(81.01)	4.22	1.15

Table S13: TCSPC lifetime fit parameters

According to our theoretical calculation we have observed a LMCT and ILCT mix state for ~370nm absorption band. It is possible that one of the components in the lifetime decay profile is coming from the LMCT excited state while the other is coming from the ligand-centered excited state.[16] (*Harrington & co-workers, Journal of the American Chemical Society **1975** 97 (21), 6029-6036)*

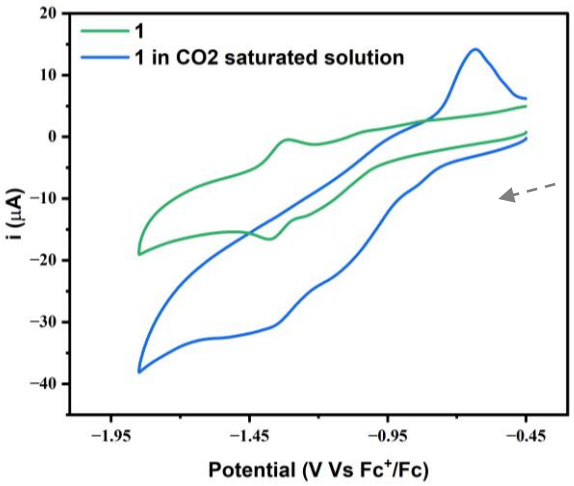

Figure S42: The CV of 0.5 mM **1** in acetonitrile and CO_2 saturated acetonitrile with 0.1 M $TBAPF_6$ WE: GC, RE: Ag/AgCl, CE: Pt wire, Scan rate: 100 mV s^{-1}

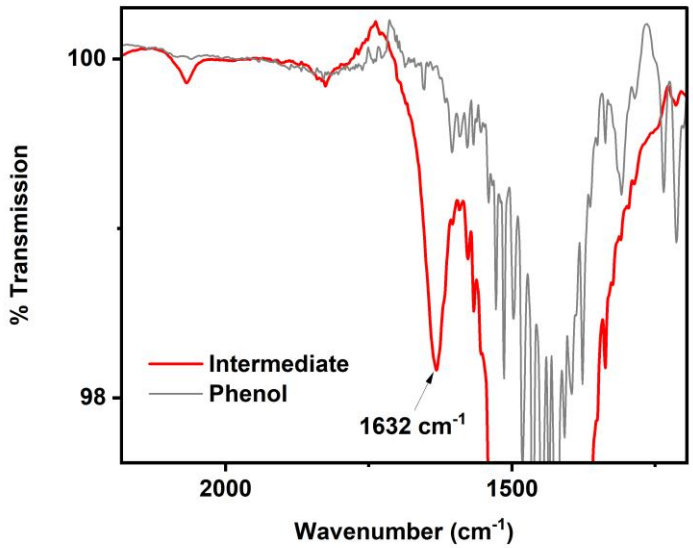

Figure S43: The infrared (IR) spectrum of a solution of complex **4** purged with CO_2 followed by the addition of p-methoxy-2,6-ditertbutylphenol (grey) at 90K to from the Cu(II)-COOH species (red) showed a peak at 1632 cm^{-1}

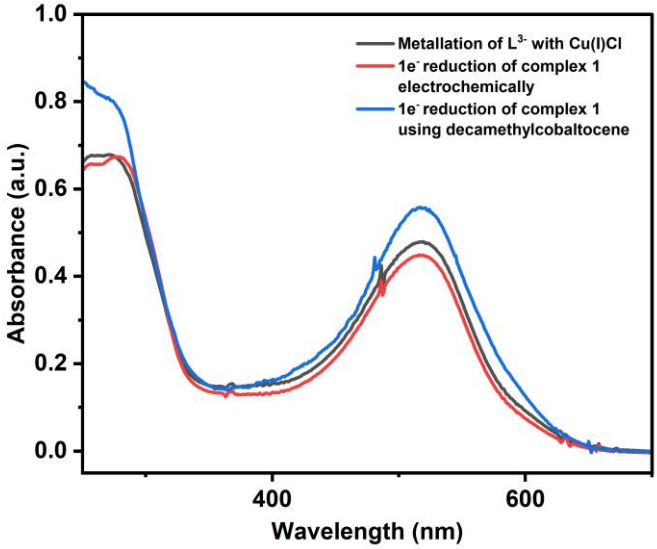

Figure S44: UV-vis absorption spectra of **4** prepared by (a) Metalation of L^{3-} with Cu(I)Cl (Black line), (b) one electron reduction of **1** electrochemically by doing CPE at -1.25V (Red line), and (c) one electron reduction of **1** using decamethylcobaltocene (Blue line)

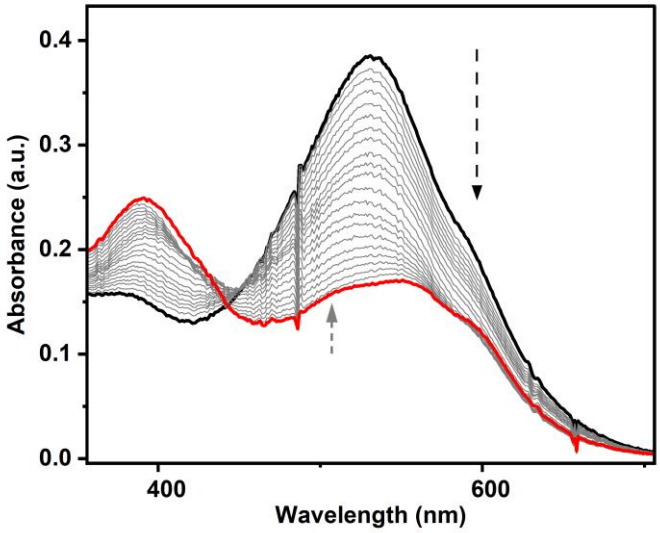

Figure S45: UV-vis absorption spectra showing the decay of species **4** (Black line) generated spectroelectrochemically by doing CPE at -1.25V (Fc^{+}/Fc). A rise of a peak ~ 506 nm (Grey arrow) signifies the formation of **3** (Red line) upon decay of **4**, thus hinting that the single electron reduced species prefers an N_3O coordination and returns to the corresponding N_3O coordinated Cu(II) species (**3**) upon reoxidation in air.

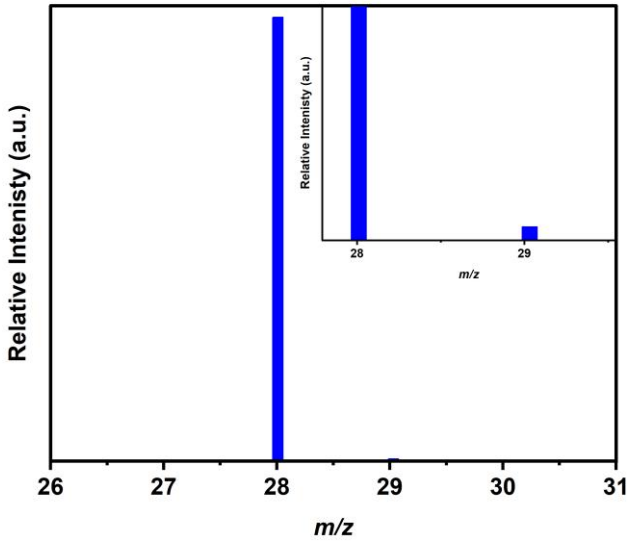

Figure S46: Mass spectra of CO (m/z: 28) detected using Gas Chromatography/ Mass Spectrometry (GC/MS) by headspace gas analysis of a CO_2 saturated 0.1 mM solution of **1** in ACN/H_2O (5% v/v) in the presence of 70 µM Et_3N upon irradiation with a 390 nm light for 2 hrs.

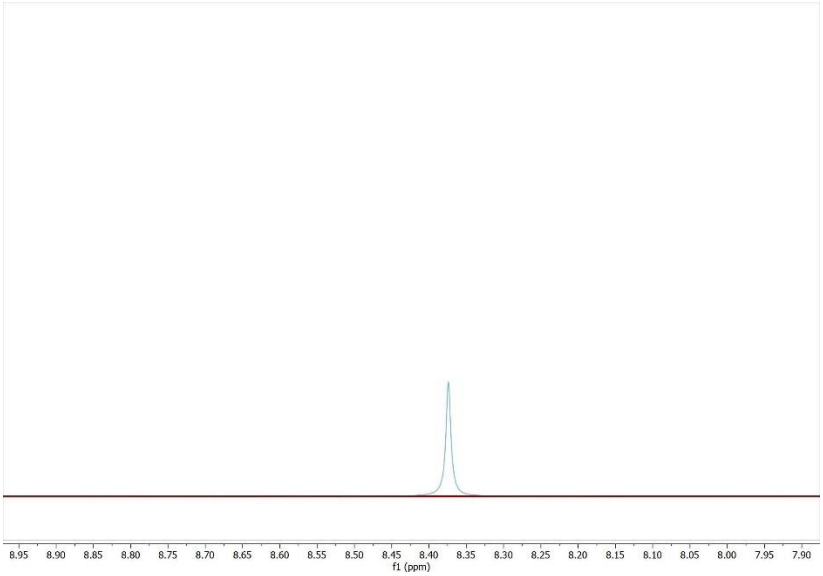

Figure S47: Solution phase product analysis with the ^{1}HNMR spectroscopy. The green line shows a formate peak as a control, and the brown line shows ^{1}HNMR of the reaction mixture extract.

Sl. No.	Function-Integrated Photocatalyst	Light (nm)	TON_{CO}	Ref. No.
1	Pyrene appended FeTPP	400-700	1220 (400nm / 24 hrs)	11
2	Fe2Na3 purpurin	450	2625 ± 334 (120 hrs)	12
3	Fe-p-TMA	λ ≥ 420	101 (102 hrs)	13
4	Cu(I)-BQXOT	450	4.69 (4 hrs)	14
5	Cu(II)purpurin	≥ 400	4.4 (1 hrs) (control exp.)	15
6	K[CuNDPA]	390	1132 (2hrs)	This Work
		400-750 (Xe lamp)	929 (2hrs)	
		427	482 (2hrs)	
		Sunlight	920 (2hrs)	

Table S14: Function-integrated first-row transition metal containing photo-catalyst-based CO_2 reduction

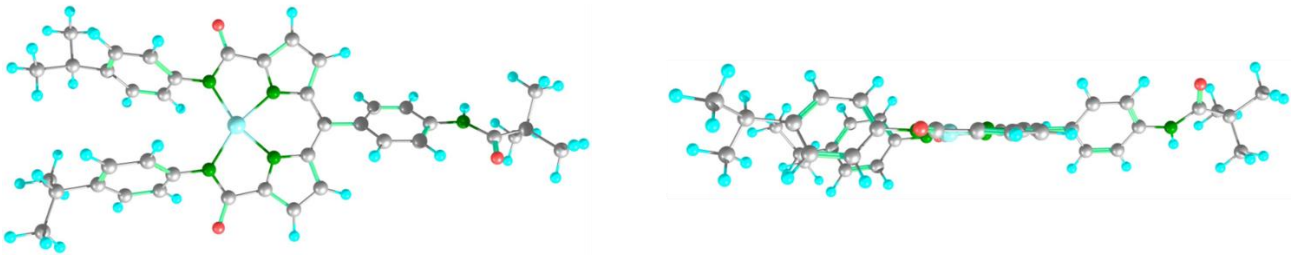

Figure S48: Optimized structure of the **1** in front side (left) and side-wise (right) view

Bonds	Crystal Bond Distances(Å)	DFT optimized Bond Distances(Å)
C-N1(pyrrole)	1.935	1.991
C-N2(pyrrole)	1.944	1.990
C-N3(amide)	1.998	2.088
C-N4(amide)	2.014	2.082

Table S15: Bond distance comparison of 1 from crystal structure and DFT optimized structure

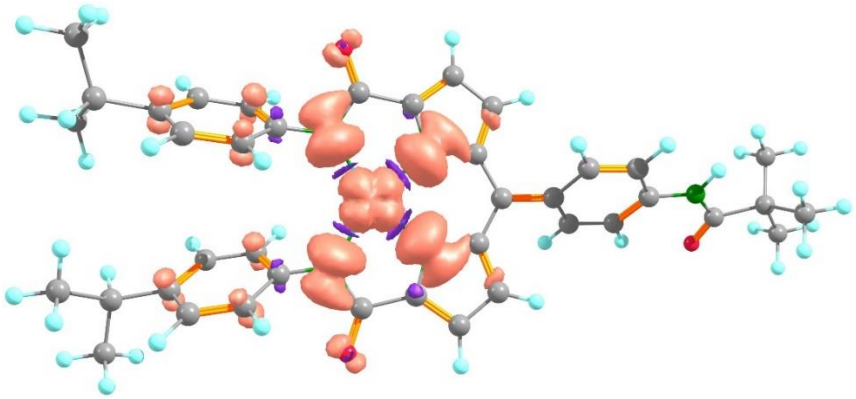

Figure S49: Spin density plot of complex **1** (isosurface value 0.003) derived from DFT calculation.

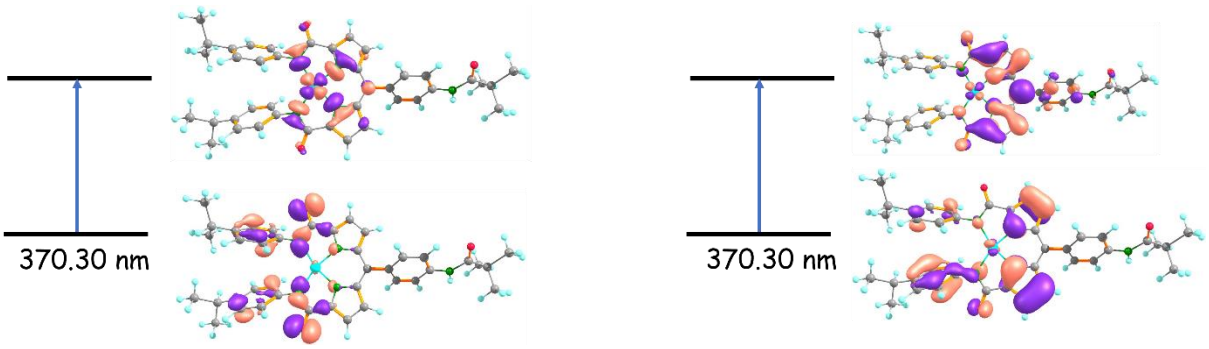

Figure S50: TD-DFT transition of **1** at 370.30 nm. Orbital plotted at 0.03 isosurface value.

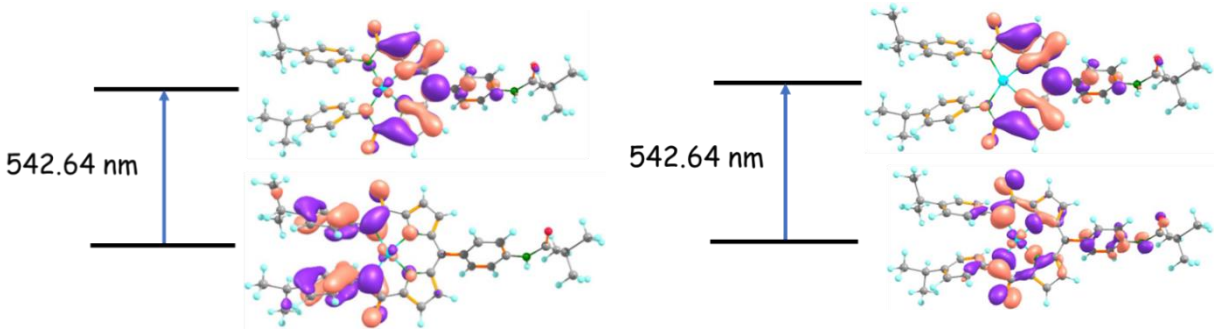

Figure S51: TD-DFT transition of **1** at 542.64 nm. Orbital plotted at 0.03 isosurface value.

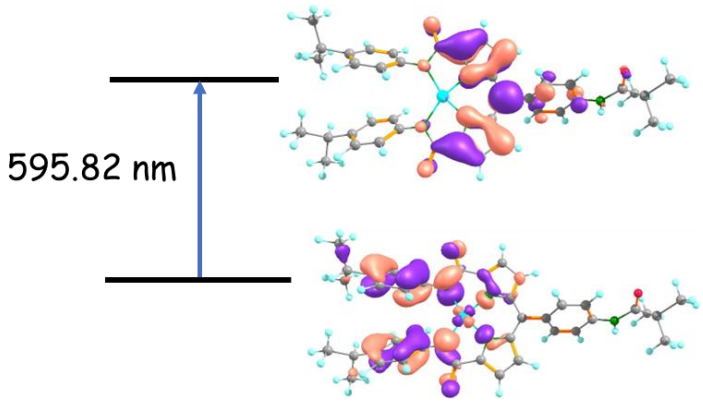

Figure S52: TD-DFT transition of **1** at 595.82 nm. Orbital plotted at 0.03 isosurface value.

DFT Studies:

K[CuNDPA](1) optimized coordinate

Spin State- 1/2, Multiplicity- 2

Cu	-0.921721000	-0.033162000	-0.036110000
O	-1.729512000	-4.097200000	0.245555000
O	-1.570110000	4.055318000	-0.320951000
O	9.063666000	1.319669000	1.201196000
N	-2.058314000	-1.787632000	0.032423000
N	0.542404000	-1.386530000	-0.011597000
N	0.597871000	1.258186000	-0.099369000
N	-1.983654000	1.761078000	-0.088827000
N	8.355617000	-0.294064000	-0.255469000
H	8.676366000	-0.997687000	-0.911380000
C	-1.314539000	-2.916452000	0.171876000
C	4.118254000	-0.139281000	-0.114088000
C	1.921179000	-1.325837000	0.049345000
C	2.494442000	2.449473000	-0.480932000
H	3.536704000	2.697975000	-0.634234000
C	6.955944000	-0.193810000	-0.165986000
C	1.414057000	3.322525000	-0.541087000
H	1.437319000	4.387005000	-0.737847000
C	-3.379749000	1.962333000	0.032900000
C	1.970335000	1.139952000	-0.200589000
C	6.200787000	-1.011453000	-1.030329000
H	6.712377000	-1.664398000	-1.733990000
C	-5.506138000	2.819438000	-0.805932000
H	-6.049480000	3.336917000	-1.593893000
C	0.152950000	-2.644504000	0.192035000

C	-1.200044000	2.859712000	-0.251073000
C	4.811714000	-0.991133000	-0.997307000
H	4.257688000	-1.622195000	-1.685732000
C	0.254592000	2.529348000	-0.304140000
C	-4.060561000	1.502880000	1.171926000
H	-3.501583000	0.989044000	1.950914000
C	2.635988000	-0.107579000	-0.086002000
C	6.276982000	0.654433000	0.727715000
H	6.835103000	1.283252000	1.407095000
C	-4.134951000	2.611751000	-0.963477000
H	-3.636217000	2.965037000	-1.861560000
C	-5.436619000	1.710679000	1.320099000
H	-5.932397000	1.348196000	2.219379000
C	2.398190000	-2.657800000	0.306373000
H	3.433171000	-2.950216000	0.428512000
C	-6.188586000	2.381860000	0.343835000
C	-3.464600000	-1.936577000	-0.042516000
C	1.284831000	-3.486352000	0.390972000
C	9.331375000	0.425352000	0.395819000
C	4.881872000	0.679108000	0.737575000
H	4.379094000	1.330964000	1.446062000
C	-4.209001000	-2.545966000	0.986690000
H	-3.693415000	-2.905735000	1.872736000
C	-6.294754000	-2.261119000	-0.256937000
C	-5.590778000	-2.707937000	0.876256000
H	-6.125616000	-3.196666000	1.688021000
C	10.784715000	0.020065000	0.050367000
C	-5.552495000	-1.627721000	-1.265327000
H	-6.064648000	-1.258898000	-2.152792000
C	-4.165853000	-1.466112000	-1.164284000
H	-3.615238000	-0.981372000	-1.967554000
C	-7.673930000	2.654301000	0.552751000
C	-7.794250000	-2.486351000	-0.414896000
H	-8.113381000	-1.909746000	-1.293790000
C	11.036535000	0.162700000	-1.469276000
H	10.436956000	-0.535796000	-2.065033000
H	12.091541000	-0.047993000	-1.682728000
H	10.817975000	1.181025000	-1.813781000
C	-8.109529000	-3.969738000	-0.697889000
H	-7.573769000	-4.329240000	-1.585306000
H	-7.819336000	-4.602633000	0.151018000
H	-7.984524000	2.074510000	1.432599000
H	1.269473000	-4.552459000	0.579546000
C	11.751395000	0.944911000	0.808166000
H	11.614219000	0.869693000	1.892079000
H	12.783461000	0.659304000	0.572492000
H	11.613005000	1.993328000	0.521855000

C	11.029777000	-1.442012000	0.493365000
H	10.833306000	-1.568599000	1.565232000
H	10.403998000	-2.156005000	-0.054615000
H	12.077530000	-1.708152000	0.307109000
C	-8.608282000	-1.984851000	0.792014000
H	-8.408452000	-0.926738000	0.999168000
H	-9.683163000	-2.095037000	0.598333000
H	-8.375474000	-2.556291000	1.699461000
C	-8.541574000	2.199247000	-0.635075000
H	-9.605636000	2.341403000	-0.405777000
H	-8.318332000	2.777375000	-1.540694000
H	-8.383493000	1.138649000	-0.864455000
C	-7.930414000	4.142528000	0.867905000
H	-8.994618000	4.315528000	1.076064000
H	-7.356066000	4.469620000	1.743639000
H	-7.645137000	4.779134000	0.020104000
H	-9.184819000	-4.110058000	-0.870668000

References:

1 W. L. F. Armarego, *Purification of Laboratory Chemicals*, 2017, 95–634.
2 M. J. Frisch, G. W. Trucks, H. B. Schlegel, G. E. Scuseria, M. A. Robb, J. R. Cheeseman, G. Scalmani, V. Barone, G. A. Petersson and H. Nakatsuji, *Wallingford, CT*.
3 A. D. Becke, *The Journal of Chemical Physics*, 1993, **98**, 5648–5652.
4 C. Lee, W. Yang and R. G. Parr, *Phys. Rev. B*, 1988, **37**, 785–789.
5 P. J. Stephens, F. J. Devlin, C. F. Chabalowski and M. J. Frisch, *J. Phys. Chem.*, 1994, **98**, 11623–11627.
6 S. H. Vosko, L. Wilk and M. Nusair, *Can. J. Phys.*, 1980, **58**, 1200–1211.
7 G. M. Sheldrick, *Acta Cryst A*, 2015, **71**, 3–8.
8 A. L. Spek, *J Appl Cryst*, 2003, **36**, 7–13.
9 L. J. Bourhis, O. V. Dolomanov, R. J. Gildea, J. a. K. Howard and H. Puschmann, *J Appl Cryst*, 2009, **42**, 339–341.
10 C. F. Macrae, I. Sovago, S. J. Cottrell, P. T. A. Galek, P. McCabe, E. Pidcock, M. Platings, G. P. Shields, J. S. Stevens, M. Towler and P. A. Wood, *J Appl Cryst*, 2020, **53**, 226–235.
11 R. J. Watts, M. J. Brown, B. G. Griffith and J. S. Harrington, *J. Am. Chem. Soc.*, 1975, **97**, 6029–6036.
11 K. Kosugi, C. Akatsuka, H. Iwami, M. Kondo, S. Masaoka, *J. Am. Chem. Soc.* **2023**, *145*, 10451–10457.

12 H. Yuan, J. Du, M. Ming, Y. Chen, L. Jiang, Z. Han, *J. Am. Chem. Soc.* **2022**, *144*, 4305–4309.
13 H. Rao, J. Bonin, M. Robert, *Chem. Commun.* **2017**, *53*, 2830–2833.
14 C. Bruschi, X. Gui, P. Rauthe, O. Fuhr, A. Unterreiner, W. Klopper, C. Bizzarri, *Chemistry A European J* **2024**, *30*, e202400765.
15 H. Yuan, B. Cheng, J. Lei, L. Jiang, Z. Han, *Nat Commun* **2021**, *12*, 1835.
16 R. J. Watts, M. J. Brown, B. G. Griffith and J. S. Harrington, *J. Am. Chem. Soc.*, 1975, **97**, 6029–6036.